Neuroendocrine Coupling of Interoceptive Bacteria-Derived Cues to Foraging Behavior in *C. elegans*

Sonia A. Boor[1,2], Joshua D. Meisel[2,3], Dennis H. Kim[1,*]

1. Division of Infectious Diseases, Department of Pediatrics, Boston Children's Hospital and Harvard Medical School, Boston, MA 02115
2. Department of Biology, Massachusetts Institute of Technology, Cambridge, MA 02139
3. Department of Molecular Biology, Massachusetts General Hospital, Boston, MA 02114

* Correspondence to dennis.kim@childrens.harvard.edu

The authors declare no competing interests.

Author contributions:

SAB: Conceptualization, Formal analysis, Validation, Investigation, Visualization, Methodology, Writing—original draft, Writing—review and editing

JDM: Investigation, Visualization, Writing – review and editing

DHK: Conceptualization, Supervision, Funding acquisition, Visualization, Methodology, Writing—original draft, Writing—review and editing

Summary

Animal internal state is modulated by nutrient intake, resulting in behavioral responses to changing food conditions. DAF-7 is a neuroendocrine TGF-beta ligand that regulates diverse food-related behaviors of *Caenorhabditis elegans,* including foraging behavior. Here, we show that in *C. elegans,* interoceptive cues from the ingestion of bacterial food inhibit the expression of DAF-7, a neuroendocrine TGF-beta ligand, from the ASJ pair of sensory neurons, whereas food deprivation in the presence of external chemosensory cues from bacteria promotes the expression of DAF-7 from the ASJ neurons. We show that SCD-2, the *C. elegans* ortholog of mammalian Anaplastic Lymphoma Kinase (ALK), which has been implicated in the central control of metabolism of mammals, functions in the AIA interneurons to regulate foraging behavior and cell-non-autonomously control the expression of DAF-7 from the ASJ neurons. Our data establish an SCD-2-dependent neuroendocrine DAF-7 gene expression feedback loop that couples the ingestion of bacterial food to foraging behavior.

Introduction

Internal states, such as fear, arousal, and hunger, are shaped by the integration of information about internal and external conditions and can result in the modulation of various physiological and behavioral outputs (Flavell et al., 2022). As animals encounter different food environments, information about internal nutritional status and external food quality can elicit transitions between internal states that either favor the exploration of new places or exploitation of the current environment. Many animals, including mammals, zebrafish, *Drosophila melanogaster*, and the roundworm *Caenorhabditis elegans,* increase exploration in response to food deprivation in order to increase chances of a food encounter (Ben Arous et al., 2009;

43 Connolly, 1966; Gutman et al., 2007; Herbers, 1981; Johnson et al., 2020; Overton & Williams,
44 2004; Russell et al., 1987). However, the mechanisms behind how animals couple changes in
45 food availability to internal states that influence foraging behavior are not well understood.
46 Insight into the cellular and organismal mechanisms governing internal states may enhance
47 understanding of the dysregulation of internal states that is thought to contribute to many human
48 psychiatric and neurological diseases (Flavell et al., 2022; Yap & Greenberg, 2018).
49 *C. elegans* forage for microbes that grow on decaying organic matter, where they
50 encounter fluctuations in not only the quantity of nutritious bacterial food available but also in
51 the quality and pathogenicity of this bacterial food (Kim & Flavell, 2020). As they navigate their
52 food environments, *C. elegans* exhibit two-state foraging and feeding behavior known as
53 roaming and dwelling (Ben Arous et al., 2009; Flavell et al., 2013; Flavell et al., 2020; Fujiwara
54 et al., 2002). On abundant nutritious food, animals spend about 80% of their time dwelling and
55 20% of their time roaming; as food becomes scarcer or lower in quality, animals increase the
56 proportion of their time roaming (Ben Arous et al., 2009). The internal states that underlie *C.*
57 *elegans* roaming and dwelling responses to changing food conditions present an experimentally
58 tractable paradigm in which to study how internal states are regulated. Furthermore, the shared
59 modulators of internal states and high degree of genetic conservation between *C. elegans* and
60 humans suggest that understanding *C. elegans* feeding and foraging behavior could have relevant
61 implications for human health and disease.
62 Aided by a complete connectome (White et al., 1986), a growing body of work has
63 examined neural circuits and their effects on foraging behavior in *C. elegans* (Ji et al., 2021;
64 Pradhan et al., 2019). The excitation or inhibition of neurons in these circuits elicits rapid
65 behavioral modulation as well as persistent behavioral states through recurrent neuronal firing.

66 Neuronal dynamics are additionally influenced by neuromodulators (Bargmann, 2012). For
67 instance, the activation of a small group of neurons can induce transitions between roaming and
68 dwelling states through conserved serotonin and pigment dispersing factor signaling (Flavell et
69 al., 2013; Ji et al., 2021). Other neuromodulators such as dopamine and octopamine can further
70 influence foraging behavior and food-dependent locomotion (Churgin et al., 2017; Oranth et al.,
71 2018; Sawin et al., 2000). Neuromodulators play a key role in mediating internal states by
72 functioning at titratable levels over longer timescales and farther distances than direct synaptic
73 signaling (Flavell et al., 2022; Sengupta, 2013). Activity-dependent gene expression in neurons
74 has been established to have key roles in the development and plasticity of neuronal circuits, but
75 less is known about how changes in neuronal gene expression may shape internal states driving
76 behavior (Yap & Greenberg, 2018). As transcription occurs on a slower timescale than neuronal
77 firing or neuromodulator release, dynamic gene expression could be important in regulating the
78 persistence of internal states.

79 We have been studying the dynamic temporal and neuron-specific expression of *daf-7*,
80 which encodes a TGF-beta ligand that is involved in the neuroendocrine regulation of a diverse
81 range of behaviors in *C. elegans*, including the dauer developmental decision, longevity,
82 metabolism, and feeding and foraging behavior (Ben Arous et al., 2009; Greer et al., 2008; Ren
83 et al., 1996; Schackwitz et al., 1996; Shaw et al., 2007). Expression of *daf-7* is restricted to a
84 limited set of sensory neurons, including the ASI neurons (Meisel et al., 2014; Ren et al., 1996;
85 Schackwitz et al., 1996). DAF-7 expression from the ASI neurons was shown to respond to
86 changing environmental conditions, such as crowding and food levels (Entchev et al., 2015; Ren
87 et al., 1996; Schackwitz et al., 1996). Previously, we observed that highly dynamic *daf-7*
88 expression can be observed in the ASJ neurons, with induction of expression in response to

89 secondary metabolites produced by pathogenic *Pseudomonas aeruginosa* PA14, which is
90 necessary for pathogen avoidance behavior (Meisel et al., 2014). In addition, we have shown that
91 upon the onset of reproductive maturity, male *C. elegans* upregulate *daf-7* expression in their
92 ASJ neurons to promote male mate-searching behavior (Hilbert & Kim, 2017).
93 Here, we have identified how the ingestion of bacterial food regulates the expression of a
94 single gene in two neurons to shape internal state dynamics driving foraging behavior in *C.*
95 *elegans*. We observed that *daf-7* transcription levels in the ASJ neurons couples foraging
96 behavior to changes in bacterial food ingestion, under the control of the highly conserved
97 receptor tyrosine kinase SCD-2/ALK. The relationship between gene transcription and
98 behavioral states across organisms is largely uncharacterized (Yap & Greenberg, 2018), and our
99 results establish a role for SCD-2/ALK-regulated dynamic neuronal gene expression in shaping
100 internal states underlying foraging behavior in response to changing nutritional conditions.
101
102 **Results**
103 **Ingested food inhibits *daf-7* expression in the ASJ neurons**
104 Our lab has previously reported that when adult hermaphrodites are fed the normal *E. coli*
105 OP50 food source, *pdaf-7::GFP* expression is restricted to the ASI chemosensory neurons
106 (Hilbert & Kim, 2017; Meisel et al., 2014). In contrast, we observed that when animals were fed
107 OP50 treated with aztreonam, an antibiotic that causes the bacteria to form inedible long strands
108 (Gruninger et al., 2008), *pdaf-7::GFP* was expressed in both the ASI and ASJ neurons (Figures
109 1A, 1C, 1D). These data suggested that ingestion of food inhibits *daf-7* expression in the ASJ
110 neurons. However, we did not observe *daf-7* expression in the ASJ neurons in the complete
111 absence of food ("Empty"), which indicated that some bacterial component of non-ingestible

112 aztreonam-treated *E. coli* OP50 was required for the induction of *daf-7* in the ASJ neurons in the
113 absence of ingested food (Figures 1A, 1C, 1D). The non-ingestible food signal that results in the
114 upregulation of *daf-7* expression in the ASJ neurons on aztreonam-treated food could be
115 diffusible, volatile, or mechanosensory. To identify the nature of the non-ingestible food cue, we
116 exposed animals to food that had been seeded on the lid of the plate (exposing animals to only
117 the volatile food cues) ("Lid") or underneath the agar (exposing animals only to diffusible food
118 cues) ("Bottom") in the absence of ingestible food and probed *daf-7* expression. We observed
119 induction of *daf-7* in the ASJ neurons when OP50 is seeded under the agar of the plates, but not
120 when present on the lid of the plate, suggesting that a bacteria-derived food signal that diffuses
121 through the agar is necessary for the induction of *daf-7* expression in ASJ in the absence of
122 ingested food. (Figures 1A-F). Thus, these data suggest that in hermaphrodites feeding on *E. coli*
123 OP50, there is an external water-soluble diffusible cue from the bacteria that stimulates *daf-7*
124 expression from the ASJ neurons, but this expression is inhibited by a second bacteria-derived,
125 interoceptive cue generated from the ingestion of bacteria (Figure 1B).

126 We next asked whether the inhibition of *daf-7* expression in the ASJ neurons by ingestion
127 of bacterial food was mediated by the early detection of ingested food or the delayed nutritional
128 effects of bacterial food consumption on organismal physiology. The kinetics of *pdaf-7::GFP*
129 induction in the ASJ neurons when animals were moved from ingestible to non-ingestible food
130 showed a rapid upregulation within 2-3 h for the GFP fluorescence in the ASJ neurons to become
131 visible (Figure 1G). Given the delay for GFP folding and accumulation to visible levels, these
132 data suggested that the absence of ingested food rapidly led to the induction of *daf-7* expression
133 in the ASJ neurons. Recent work has described the interoceptive sensing of ingested food by the
134 acid-sensing ion channels (ASICs) encoded by *del-3* and *del-7*, which are expressed in the minor

135 neurites of the NSM neurons where they detect food in the pharynx and mediate behavioral
136 slowing upon encountering food (Rhoades et al., 2019). We observed that *del-3;del-7* animals
137 expressed *daf-7* in the ASJ neurons even on ingestible food (Figure 1H). These observations are
138 consistent with the hypothesis that the detection of an interoceptive ingested food signal in the
139 pharynx, mediated by DEL-3 and DEL-7, inhibits *daf-7* expression in the ASJ neurons.
140

141 ***daf-7* expression in the ASJ neurons promotes roaming behavior**

142 Next, we sought to understand how changes in *daf-7* expression in the ASJ neurons in
143 response to changing food conditions might modulate food-dependent behavior. Feeding *C.*
144 *elegans* alternate between two distinct behavioral states known as roaming and dwelling (Ben
145 Arous et al., 2009; Fujiwara et al., 2002). On nutritious food, wild-type animals spend most of
146 their time dwelling, a feeding state marked by a low movement speed and high body bending
147 angle. As food conditions worsen, animals will decrease the fraction of time dwelling and
148 increase the fraction of time roaming, a foraging state marked by high speed and low curvature
149 (Ben Arous et al., 2009). Prior genetic analysis of roaming and dwelling has revealed a role for
150 DAF-7 in promoting roaming behavior, with *daf-7* animals spending a decreased fraction of time
151 roaming compared to wild-type animals (Ben Arous et al., 2009). Using both worm-tracking
152 software to quantify roaming and dwelling (*WormLab*, 2020) and an exploration assay to
153 measure the general activity levels of animals ((Flavell et al., 2013), see Materials and Methods),
154 we observed that *daf-7(e1372)* and *daf-7(ok3125)* animals spent a markedly decreased
155 proportion of time in the roaming state than wild-type animals, consistent with these prior
156 findings (Figure 2A). To determine whether we could detect modulation of roaming and
157 dwelling behaviors caused by changes in *daf-7* expression in the ASJ neurons, we adopted two

158 complementary approaches. First, we found that in a *daf-7(ok3125)* background, rescue of *daf-7*
159 cDNA under the ASJ-specific *trx-1* promoter partially restored the fraction of time animals spent
160 in the roaming state (Figure 2B). Second, we examined exploratory behavior in animals that had
161 *daf-7* deleted in the ASJ neurons, using a floxed allele of *daf-7* and Cre expressed under the *trx-1*
162 promoter. We found that animals with an ASJ-specific *daf-7* deletion explored less of the lawn
163 than animals with wild-type expression of *daf-7* (Figure 2C).

164 The relationships between ingested food and *daf-7* expression in the ASJ neurons, *daf-7*
165 expression in the ASJ neurons and roaming, and roaming and amount of food ingested suggest a
166 neuroendocrine gene expression positive-feedback loop that couples the ingestion of bacterial
167 food to the modulation of foraging behavior through *daf-7* expression in the ASJ neurons (Figure
168 2D). When animals are on abundant edible food, the ingestion of this food inhibits *daf-7*
169 expression in the ASJ neurons and attenuates the proportion of time in the roaming state. When
170 animals are removed from edible food, upregulation of *daf-7* expression in the ASJ neurons
171 promotes an increased proportion of time in the roaming state. We hypothesized that this
172 transcriptional feedback loop might function in the persistence of internal states underlying
173 roaming and dwelling behaviors, so we measured the duration of roaming and dwelling states in
174 animals lacking DAF-7 signaling.

175 Representative trace files of wild-type, *daf-7(e1372),* and *daf-7(ok3125)* animals show
176 how DAF-7 can influence roaming and dwelling state duration (Figure 2E). Quantification of
177 state duration across multiple animals revealed that *daf-7* animals exhibited shortened roaming
178 states relative to wild-type animals as predicted by the positive feedback loop (Figure 2F). We
179 did not observe a difference in dwelling state duration among the genotypes examined, although

180 we suspect the wide variation dwelling state durations exhibited by animals precluded the
181 detection of a statistically significant difference with our analysis.
182
183 **Known modulators of foraging behavior also regulate *daf-7* expression**
184 The positive-feedback loop supported by our data (Figure 2D) implies that *daf-7*
185 expression in the ASJ neurons could be increased in genetic backgrounds favoring roaming
186 behavior and hence a diminished ingestion of bacterial food. Serotonin has been shown to
187 promote long dwelling states, and thus animals with mutations in *tph-1,* the gene encoding the
188 enzyme that catalyzes the rate-limiting step of serotonin biosynthesis, spend a greater proportion
189 of their time in the roaming state (Figure 3A) (Flavell et al., 2013; Ji et al., 2021). Consistent
190 with the correlation between *daf-7* expression in the ASJ neurons and roaming, we see that *tph-*
191 *1(n4622)* animals constitutively express *daf-7* in the ASJ neurons on both ingestible and non-
192 ingestible food, with this *daf-7* expression retaining sensitivity to changes in food environments
193 (Figure 3B).
194 Pigment dispersing factor (PDF) signaling has also been previously shown to modulate
195 roaming and dwelling behavior, with animals carrying loss-of-function mutations in the PDF
196 receptor gene *pdfr-1* showing a decreased fraction of their time in the roaming state than wild-
197 type animals (Figure 3C) (Flavell et al., 2013; Ji et al., 2021). Consistent with the correlation
198 between roaming and *daf-7* expression in ASJ, we observed that animals with loss-of-function
199 mutations in *pdfr-1* do not upregulate *daf-7* transcription in the ASJ neurons on non-ingestible
200 food (Figure 3D). From a screen done in parallel to this work, we recovered a putative gain-of-
201 function allele of *pdfr-1*, *syb3826,* carrying a S325F substitution (Boor, 2022). We observed that
202 *pdfr-1(syb3826)* animals exhibited increased roaming behavior compared with wild-type animals

203 (Figure 3C) and constitutive expression of *daf-7* in the ASJ neurons when fed ingestible food,
204 which is further upregulated on non-ingestible food (Figure 3D).
205
206 **SCD-2 controls *daf-7* expression in the ASJ neurons and roaming**
207 To identify additional genetic factors involved in coupling the ingestion of food to *daf-7*
208 expression in the ASJ neurons and its subsequent effect on roaming, we were guided by the
209 isolation of an allele of *hen-1, qd259,* in a screen for genes regulating the expression of *daf-7*
210 from the ASJ neurons in response to *P. aeruginosa*. Through genomic rescue experiments, we
211 confirmed that the *hen-1* mutation was the causative lesion in this strain, and animals with
212 mutations in *scd-2,* encoding the receptor of HEN-1, share this phenotype (Figure 4A). SCD-2
213 has characterized for its role in the food-dependent developmental arrest known as dauer
214 diapause (Reiner et al., 2008), and Anaplastic Lymphoma Kinase (ALK), the human ortholog of
215 SCD-2, has been implicated in metabolic phenotypes in humans, mice, and *Drosophila* (Orthofer
216 et al., 2020). Taken together, these observations led us to question if SCD-2 might be involved in
217 the regulation of *daf-7* expression in the ASJ neurons in response to changes in food ingestion.
218 We found that animals with loss-of-function alleles of either *scd-2* or *hen-1* showed reduced
219 upregulation of *daf-7* in the ASJ neurons in response to non-ingestible food compared to wild-
220 type animals, implicating SCD-2 in this *daf-7* expression response (Figures 4B and 4D).
221 To further examine the role of SCD-2 mediating the *daf-7* expression response to
222 ingested food, we generated a gain-of-function allele. Gain-of-function point mutations in ALK
223 are associated with neuroblastoma and most often occur in the kinase domain, with 85% of all
224 ALK point mutations seen at either F1174 or R1275 (Franco et al., 2013). F1174L, the most
225 common point mutation, results in ALK autophosphorylation and cytokine-independent growth

226 (Chen et al., 2008; George et al., 2008; Hallberg & Palmer, 2013; Holla et al., 2017; Janoueix-
227 Lerosey et al., 2008). Analysis of a sequence alignment of SCD-2 and ALK revealed that F1174
228 in ALK was conserved as F1029 in SCD-2, and we were able to create a gain-of-function allele
229 of *scd-2* by engineering a F1029L substitution (*scd-2(syb2455)*) (Figure 4C) (Boor, 2022). To
230 infer whether SCD-2 activity was sufficient to induce expression of *daf*-7 in the ASJ neurons in
231 the absence of ingestible bacterial food, we examined the gain-of-function *scd-2(syb2455)*
232 mutant and observed that these animals constitutively expressed *daf-7* in the ASJ neurons even in
233 the presence of ingestible food (Figure 4D). We further observed that the magnitude of
234 upregulation of *daf-7* expression in the ASJ neurons when animals were moved from ingestible
235 food to non-ingestible food was reduced in *scd-2(syb2455)* to levels only about one-fourth of
236 those seen in wild-type animals (Figure 4D). In contrast, these *scd-2(syb2455)* gain-of-function
237 animals still show robust upregulation of *daf-7* expression in the ASJ neurons when exposed to
238 *P. aeruginosa,* supporting a direct role for SCD-2 in the response to ingested food rather than a
239 global control of *daf-7* expression in the ASJ neurons (Figure 4A).
240 Expression of *scd-2* cDNA under the AIA-specific *gcy-28.d* promoter has been shown to
241 be sufficient to rescue behavioral phenotypes of *scd-2* mutants that have been attributed to a role
242 for AIA-expressed SCD-2 in sensory integration (Shinkai et al., 2011). To ask whether SCD-2
243 could be functioning in the AIA neurons to regulate *daf-7* expression in the ASJ neurons, we
244 generated a strain with the coding sequence of SCD-2 floxed and introduced a transgene
245 expressing Cre under the *gcy-28.d* promoter. Compared to animals containing a floxed *scd-2*
246 allele without Cre, animals with AIA-specific Cre expression resulting in AIA-specific deletion
247 of *scd-2* showed reduced upregulation of *daf-7* expression in the ASJ neurons in response to non-

248 ingestible food, suggesting that SCD-2 activity in the AIA neurons acts cell-non-autonomously
249 to control *daf-7* expression in the ASJ neurons (Figure 4E).
250 Our finding that SCD-2 regulates the *daf-7* expression in response to ingested food
251 predicts that SCD-2 would also promote roaming behavior. Consistent with this hypothesis, we
252 observed that animals with loss-of-function mutations in *scd-2* spent a lower proportion of time
253 roaming and explored less of the lawn in an exploration assay than wild-type animals (Figure
254 4F). Animals with a loss-of-function allele of *hen-1* also roamed less than wild type (Figure 4F).
255 Furthermore, as predicted by their regulation of *daf-7* expression in the ASJ neurons, *scd-2* and
256 *hen-1* animals exhibit shorter roaming states and unchanged dwelling state durations compared
257 to wild-type animals (Figure 4G). When we examined the roaming and dwelling behavior of *scd-*
258 *2(syb2455)* gain-of-function animals, we found that these mutants showed increased roaming
259 behavior and lawn exploration as compared to wild-type animals and exhibited longer roaming
260 states (Figure 4H and 4I). As with the regulation of *daf-7* expression in the ASJ neurons, we
261 observed that Cre-lox-mediated deletion of *scd-2* specifically in the AIA neurons reduced both
262 roaming and exploration compared to floxed *scd-2* animals without Cre, suggesting that SCD-2
263 functions in the AIA interneurons to promote roaming behavior (Figure 4J).
264
265 **A neuronal gene expression corelate of internal state dynamics driving foraging behavior**
266 Considering our positive feedback model, we reasoned that conditions under which we
267 have observed *daf-7* expression in the ASJ neurons would correlate with increased roaming
268 behavior. Previous work from our lab has shown that upon reaching reproductive maturity, male
269 *C. elegans* induce *daf-7* expression in their ASJ neurons, which contributes to male mate-
270 searching behavior (Hilbert & Kim, 2017). Consistent with the behaviors that have

271 been reported for males and hermaphrodites in bacterial food-leaving assays, we observed that
272 wild-type males spend a greater proportion of their time in the roaming state than hermaphrodites
273 (Figure 5B). We also observed that the *daf-7* expression in the ASJ neurons in males was
274 sensitive to the inhibitory effects of ingested food, although the magnitude of the fold increase in
275 *daf-7* expression from the ASJ neurons was about half that observed for hermaphrodites (Figure
276 5A).

277 We have also previously reported an upregulation in *daf-7* expression in the ASJ neurons
278 when animals are on pathogenic *P. aeruginosa* PA14 in response to specific secondary
279 metabolites phenazine-1-carboxamide and pyochelin (Figure 5C) (Meisel et al., 2014). Analysis
280 of roaming and dwelling on PA14 revealed that animals significantly increase the fraction of
281 their time in the roaming state on PA14 compared to nonpathogenic *E. coli* OP50 (Figure 5D).
282 We observed that upon exposure to the nonpathogenic PA14 mutant ΔgacA, which results in an
283 intermediate level of *daf-7* expression in the ASJ neurons (Figure 5C) (Meisel et al., 2014),
284 animals roamed an intermediate amount between animals on OP50 and pathogenic PA14 (Figure
285 5D).

286

287 **Discussion**

288

289 **A neuroendocrine gene expression feedback loop couples the ingestion of bacterial food to**
290 **foraging behavior**

291 The data we present here support a model in which bacterial food ingestion regulates
292 roaming and dwelling behavior in part via SCD-2-dependent *daf-7* expression in the ASJ
293 neurons. Our identification of the AIA neurons as the site of SCD-2 action is consistent with a

294 role for the AIA neurons in relaying food signals in other contexts. AIA has been characterized
295 as a downstream synaptic target of multiple food sensory neurons to integrate information about
296 the food environment and influence chemoreceptor expression in other neurons (Dobosiewicz et
297 al., 2019; McLachlan et al., 2022).

298 We have observed that the expression of *daf-7* in the ASJ neurons responds to two
299 opposing food cues. An interoceptive cue derived from the sensation of ingested food in the
300 pharynx inhibits the expression of *daf-7* in the ASJ neurons, while the presence of a diffusible
301 non-ingested food cue induces the expression of *daf-7* in the ASJ neurons (Figure 1B). In the
302 presence of both food cues, as on abundant ingestible food, the interoceptive food signal is
303 epistatic to the external food signal, promoting exploitation of the current food environment with
304 low levels of *daf-7* expression in the ASJ neurons. Our identification of two opposing food cues
305 is consistent with findings from Wexler et al., who reported that aztreonam-treated bacteria could
306 restore *daf-7* expression in the ASJ neurons of starved males, indicative of an external food cue
307 that is upregulating *daf-7* expression in the ASJ neurons (Wexler et al., 2020).

308 As discussed above, the relationship between foraging behavior, food ingestion, and
309 SCD-2-dependent *daf-7* expression has led us to posit a positive-feedback loop that couples food
310 ingestion with foraging behavior (Figure 2D). As animals in a patchy food environment
311 encounter a region with less edible food, our model predicts that a reduction of ingested food
312 would result in *daf-7* expression induction in the ASJ neurons via SCD-2. This increase in *daf-7*
313 expression is correlated with an internal state that favors roaming. As animals roam, they ingest
314 less bacteria, further promoting SCD-2-dependent *daf-7* expression in the ASJ neurons,
315 stabilizing a roaming-prone state. Once a roaming animal encounters edible food and begins to
316 eat, the interoceptive sensation of food in the pharynx results in a downregulation of *daf-7*

317 expression in the ASJ neurons, promoting a dwelling state in which the animal can continue to
318 eat. As additional food is ingested, this further reduces *daf-7* expression in the ASJ neurons,
319 stabilizing this internal state that favors dwelling.

320 A number of recent studies in *C. elegans* point to a key role for neuronal transcriptional
321 responses in the regulation of behavioral plasticity in response to changing environmental stimuli
322 such as food and temperature (Harris et al., 2023; Kyani-Rogers et al., 2022; Ryan et al., 2014;
323 Wexler et al., 2020). For example, differential expression of the diacetyl-sensing chemoreceptor
324 ODR-10 in the AWA neurons in response to changing food conditions, which functions
325 downstream of *daf-7* expression in the ASJ neurons of males, has been shown to modulate food-
326 leaving mate-searching behavior (Ryan et al., 2014; Wexler et al., 2020). We anticipate that the
327 characterization of neuron-specific transcriptional changes that are correlated with *daf-7*
328 expression in the ASJ neurons may yield additional mechanistic insights into how changing
329 environmental and endogenous ingested bacterial food levels modulate internal states driving
330 foraging behavior.

331

332 **SCD-2/ALK controls a neuroendocrine response to the ingestion of bacterial food**

333 Here, we show that *daf-7* expression in the ASJ neurons is regulated by the receptor
334 tyrosine kinase SCD-2. SCD-2 and its ligand, HEN-1, have been implicated sensory integration,
335 associative learning, and memory (Ishihara et al., 2002; Shinkai et al., 2011; Wolfe et al., 2019),
336 and SCD-2 was initially characterized for its role in regulating dauer formation, a
337 developmentally arrested state induced by stressful growth conditions, including lack of
338 nutritious food (Golden & Riddle, 1982, 1984a, 1984b, 1984c; Inoue & Thomas, 2000; Reiner et
339 al., 2008). SCD-2 is the *C. elegans* ortholog of Anaplastic Lymphoma Kinase (ALK). In humans,

340 *ALK* is expressed primarily in the nervous system and influences cell proliferation,
341 differentiation, and survival in response to external stimuli (Iwahara et al., 1997). Genetic
342 translocations resulting in gene fusions are common in *ALK*-dependent human cancers, including
343 non-small cell lung cancer (NSSLC), diffuse large B cell lymphoma (DLBCL), squamous cell
344 carcinoma (SCC), and renal cell carcinoma (RCC) (Hallberg & Palmer, 2013; Holla et al., 2017;
345 Morris et al., 1994). Recent studies have suggested a physiological role for ALK in the neuronal
346 control of metabolism. A genome-wide association study (GWAS) looking for genetic variants
347 associated with thinness identified a variant in the first intron of *ALK* (Orthofer et al., 2020).
348 Additional studies in *Drosophila* and mice have further implicated ALK in triglyceride
349 accumulation, starvation survival, and metabolic response to high-fat diets (Cheng et al., 2011;
350 Orthofer et al., 2020; Woodling et al., 2020).

351 We have observed a role for SCD-2 in regulating foraging behavior and neuroendocrine
352 gene expression in response to changing food conditions. We and others have observed that
353 animals with loss-of-function mutations in *scd-2* behave as if they are in the constant presence of
354 ingested "good" food; *scd-2* animals dwell more, reduce upregulation of *daf-7* expression in the
355 ASJ neurons in the absence of ingested food, and fail to enter dauer under poor food conditions
356 (Reiner et al., 2008). In contrast, animals with the gain-of-function *scd-2(syb2455)* allele act like
357 animals exposed to "bad" food conditions, as evidenced by increased roaming, constitutive
358 expression of *daf-7* in their ASJ neurons, and food-independent constitutive dauer entry (Boor,
359 2022).

360 The role for SCD-2 in regulating the physiological response to ingested food in *C.*
361 *elegans* is consistent with the growing body of work tying ALK and its orthologs to thinness and
362 metabolic phenotypes in humans, mice, and *Drosophila* (Cheng et al., 2011; Orthofer et al.,

363 2020; Woodling et al., 2020). Our observations of *scd-2 C. elegans* are consistent with
364 phenotypes seen in *ALK*$^{-/-}$ mice and *Alk* RNAi *Drosophila*, including increased energy
365 expenditure and reduced triglyceride accumulation (Orthofer et al., 2020). Since the phenotypes
366 of *scd-2* animals are associated with abundant food in *C. elegans,* we might expect these *ALK*$^{-/-}$
367 mice and *Alk* RNAi *Drosophila* to mimic animals that are constantly eating and engage in
368 compensatory mechanisms of increased energy expenditure and triglyceride metabolism. Further
369 characterization of the mechanisms by with SCD-2 and ALK regulate food-dependent behavior,
370 gene expression, and metabolism could reveal new factors governing body weight and have
371 implications in the treatment and prevention of obesity.
372
373 ***daf-7* expression in the ASJ neurons is correlated with internal state favoring exploration**
374 The response of *daf-7* expression in the ASJ neurons to changes in food conditions and
375 its effect on foraging behavior provides an example of the influence of gene expression on
376 internal states. We have identified a transcriptional switch of one gene in two cells that can
377 influence foraging behavior in a manner as equally simple as but on a longer time scale than
378 neuronal firing (Figure 5E). This *daf-7*-expressing, pro-roaming internal state might drive other
379 exploratory behaviors that our lab and others have observed under conditions were *daf-7* is
380 expressed in the ASJ neurons. Male *C. elegans* have been observed to upregulate the expression
381 of *daf-7* in their ASJ neurons upon reaching reproductive maturity, and this *daf-7* expression has
382 been implicated in driving mate-searching behavior (Hilbert & Kim, 2017). Males must find a
383 hermaphrodite mate to reproduce – a requirement not shared by hermaphrodites – and they often
384 must leave food to do so. The constitutive expression of *daf-7* in the ASJ neurons of adult males
385 could be due to a reduced sensitivity to ingested food allowing for prioritization of searching for

386 a mate over feeding. This is consistent with our observation that *daf-7* expression in the ASJ
387 neurons is upregulated less in response to non-ingestible food in males than in hermaphrodites.
388 Similarly, our lab has previously reported that two secondary metabolites of pathogenic
389 *P. aeruginosa* can result in the upregulation of *daf-7* expression in the ASJ neurons, which
390 contributes to pathogen avoidance behavior (Meisel et al., 2014). The results presented here
391 suggest that perhaps these secondary metabolites are tapping into this foraging circuit and
392 overriding other inputs that regulate *daf-7* expression in the ASJ neurons to promote the animals
393 moving away from the pathogen in a manner like roaming animals seeking nutritious food. In the
394 natural environment of *C. elegans*, pathogenic and nutritious bacteria coexist, and animals must
395 employ mechanisms to avoid infection while still obtaining adequate nutrition. Low levels of
396 nutritious food, the presence of pathogen, or an absence of mates each represents a suboptimal
397 environment and may induce a common internal state that promotes exploration and enhances
398 the chances of encountering more favorable conditions.
399
400
401 **Materials and Methods**
402 ***C. elegans* strains:** *C. elegans* was maintained on *E. coli* OP50 as previously described
403 (Brenner, 1974). Daf-c strains were grown at 16˚C. See Table 1 for a complete list of strains used
404 in this study.
405 **Design of potential *scd-2* gain-of-function alleles:** We performed a protein alignment of *C.*
406 *elegans* SCD-2 and human ALK in NCBI BLAST (Figure 4C). Using a list of known oncogenic
407 ALK mutations (Holla et al., 2017), we screened these residues for conservation or similarity
408 between the *C. elegans* and human protein sequences. Genome editing was done by SunyBiotech

409 using CRISPR technology. Alleles were evaluated in a dauer assay for a gain-of-function Daf-c
410 phenotype, and validated in trans-heterozygote analysis with *scd-2(sa249)* for a dominant
411 phenotype (Boor, 2022).
412 **Preparation of food condition plates:** Unless otherwise indicated, all assays were performed on
413 NGM plates with no peptone. Aztreonam-treated bacteria was prepared as previously reported
414 (Gruninger et al., 2008), and 40 µL aztreonam-treated food was added to plates containing 10
415 µg/mL aztreonam. "Fed" plates for *daf-7* quantification were seeded with 40 µL OP50 grown
416 overnight in a shaking LB culture at 37˚C. "Bottom" plates were seeded with 250 µL OP50, and
417 the agar was inverted with a spatula immediately prior to adding animals. "Lid" plates were
418 prepared by pouring a spot of NGM agar on the inside of the lid of the plate and seeding 100 µL
419 of OP50 on to the spot. PA14 was grown as previously described and seeded onto SKA plates, as
420 were *E. coli* OP50 controls for these experiments (Meisel et al., 2014).
421 ***pdaf-7::gfp* quantification assays:** Plates of gravid animals were bleached and eggs were
422 dropped onto NGM plates seeded with OP50 and grown at 20˚C for 67 hours, unless otherwise
423 noted. On the day of imaging, 15-30 day one adult animals were transferred by picking to assay
424 plates, where they were incubated for 5 hours at 20˚C. Animals to be imaged were mounted on
425 glass slides with agarose pads and 50 mM sodium azide or 5 mM Levamisole. All imaging for
426 pictures were conducted on the Zeiss Axioimager Z1. Quantification of GFP brightness was
427 derived from maximum fluorescence values within the ASJ neurons in FIJI.
428 **Exploration assay:** The exploration assay was performed loosely as previously described with
429 several modifications (Flavell et al., 2013). Thirty-five millimeter NGM plates with no peptone
430 were seeded with 500 µL OP50 grown overnight in LB so that the lawn covered the entire
431 surface of the plate. On the day of the assay, one day-one adult animal was placed on the plate

432 and allowed to explore for two hours before being removed. The plate was then superimposed on
433 a grid of 3.5 mm squares and the number of squares crossed by the *C. elegans* tracks was
434 manually counted.
435 **Roaming/dwelling assay:** Animals were egg-laid and grown to day-one adults. 10 cm NGM
436 plates without peptone were seeded with 2 mL stationary phase *E. coli* OP50 grown overnight in
437 LB. Assays were performed with ~20 animals inside a 6 cm copper ring placed in the center of
438 the seeded plate. After one hour for the animals to adjust to their new environment, videos were
439 recorded at 3.75 frames per second for 1.5-3 hours. Videos were analyzed using MBF
440 Biosciences WormLab software (*WormLab*, 2020).
441 Measurements of speed and bending angle (midpoint) were averaged over 10 second
442 intervals, and values for each 10-second interval were plotted on a scatter plot of speed (µm/sec)
443 vs. bending angle (degrees). Quantification of fraction of time spent roaming or dwelling was
444 done by segregating the points of the scatter plots by a horizontal line whose placement was
445 based on the distribution of points in the control condition for each experiment. Values for this
446 speed cutoff ranged from y=7 to y=12. Points falling above the line were classified as roaming,
447 and those below the line were classified as dwelling. The fraction of time spent roaming was
448 calculated for each animal based off the speed cutoff. Outliers were removes using a ROUT test
449 with Q = 1%. The durations of roaming and dwelling states were determined manually by
450 analyzing average speed values for successive ten-second intervals. Only states lasting longer
451 than five intervals (fifty seconds) were considered.
452 **Statistics:** All statistical analysis was performed using the GraphPad Prism software (Graphpad
453 Prism, RRID: SCR_002798). Statistical tests used are indicated in each figure legend.
454

Acknowledgements: We thank Bob Horvitz and the Caenorhabditis Genetics Center, which is funded by the NIH Office of Research Infrastructure Programs (P40 OD010440), for strains, and Cori Bargmann for Cre plasmids. We thank current and past members of the Kim lab for discussions. Finally, we acknowledge financial support from NIH grant R35GM141794.

Strain Name	**Genotype**	**Source**
N2	Wild type	Caenorhabditis Genetics Center (CGC)
JT249	*scd-2(sa249)*	CGC
RB783	*scd-2(ok565)*	CGC
JC2154	*hen-1(tm501)*	CGC
PHX2455	*scd-2(syb2455)*	This study/SunyBiotech
FK181	*ksIs2[pdaf-7::gfp; rol-6(su1006)]*	CGC
ZD2540	*ksIs2; scd-2(sa249)*	This study
ZD930	*ksIs2; scd-2(ok565)*	This study
ZD918	*ksIs2; hen-1(tm501)*	This study
ZD2605	*ksIs2; scd-2(syb2455)*	This study
CB1372	*daf-7(e1372)*	CGC
ZD715	*daf-7(ok3125)*	(Meisel et al., 2014)
ZD695	*daf-7(ok3125);qdEx34[ptrx-1::daf-7;pges-1::GFP]*	(Meisel et al., 2014)
ZD696	*daf-7(ok3125);qdEx35[ptrx-1::daf-7;pges-1::GFP]*	(Meisel et al., 2014)
ZD2632	*ksIs2; del-3(ok2613);del-7(ok1187)*	This study
MT14984	*tph-1(n4622)*	Horvitz Lab
ZD667	*ksIs2; tph-1(n4622)*	This study
ZD2079	*pdfr-1(ok3425)*	(Hilbert & Kim, 2018)
PHX3826	*pdfr-1(syb3826)*	This study/SunyBiotech
ZD1987	*ksIs2; pdfr-1(ok3425); him-5(e1490)*	(Hilbert & Kim, 2018)
ZD2633	*ksIs2; pdfr-1(syb3826); him-5(e1490)*	This study
ZD2721	*scd-2(syb5845 syb6052) Backcrossed x2*	This study
ZD2722	*daf-7(syb5855 syb5965) qdEx[ptrx-1::Cre; pofm-1::gfp] Backcrossed x2*	This study
ZD2752	*scd-2(syb5845 syb6052); ex[gcy-28.dp::cre; ofm-1p::gfp]*	This study
ZD2766	*scd-2(syb5845 syb6052); ex[gcy-28.dp::cre; ofm-1p::gfp]; ksIs2*	This study
ZD1005	*him-5(e1390); ksIs2*	(Hilbert & Kim, 2017)

461
462 **Table 1.** Complete list of *C. elegans* strains used in this study.

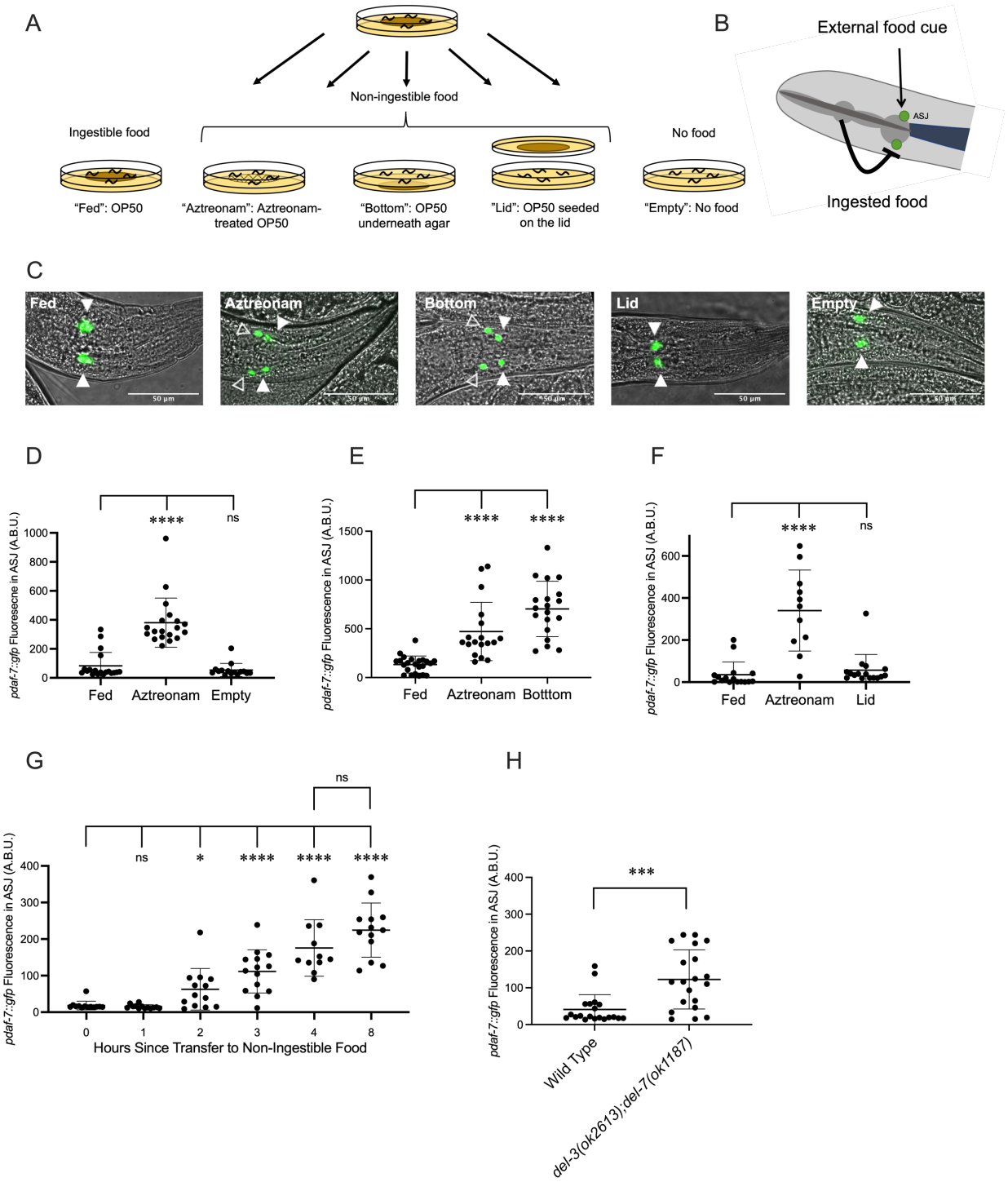

Figure 1. Ingestion of bacterial food inhibits *daf-7* expression in the ASJ neurons.

A. Schematic of experimental exposure to varied food conditions. Animals were grown to adulthood on edible *E. coli* OP50, then transferred to various experimental food conditions: "Fed": *E. coli* OP50; "Aztreonam": OP50 treated with aztreonam; "Bottom":

468 OP50 was seeded underneath the agar of the plate; “Lid”: Animals placed on agar with
469 no food but where food was seeded on a spot of agar on the inside of the lid of the plate;
470 “Empty”: no food.

471 B. Model for the convergence of external and ingested food signals on *daf-7* expression in
472 the ASJ neurons.

473 C. *pdaf-7::gfp* expression pattern in animals under different food conditions, from left to
474 right: “Fed,” “Aztreonam,” “Bottom,” “Lid,” “Empty.” Filled triangles indicate the ASI
475 neurons; open triangles indicate the ASJ neurons. Scale bar indicates 50 µm.

476 D. E. F. Maximum fluorescence values of *pdaf-7::gfp* in the ASJ neurons of adult animals
477 under various food conditions. Each point represents an individual animal, and error bars
478 indicate standard deviation. ****$p<0.0001$, ns not significant as determined by an
479 unpaired two-tailed t-test.

480 G. Maximum fluorescence values of *pdaf-7::gfp* in the ASJ neurons of adult animals at
481 various time points after being moved from “Fed” to “Bottom” conditions. Each point
482 represents an individual animal, and error bars indicate standard deviation.
483 ****$p<0.0001$, * $p<0.05$, ns not significant as determined by an unpaired two-tailed t-
484 test.

485 H. Maximum fluorescence values of *pdaf-7::gfp* in the ASJ neurons of adult wild type and
486 *del-3(ok2613); del-7(ok1187)* under “Fed” conditions. Each point represents an
487 individual animal, and error bars indicate standard deviation. ***$p<0.001$, as determined
488 by an unpaired two-tailed t-test.

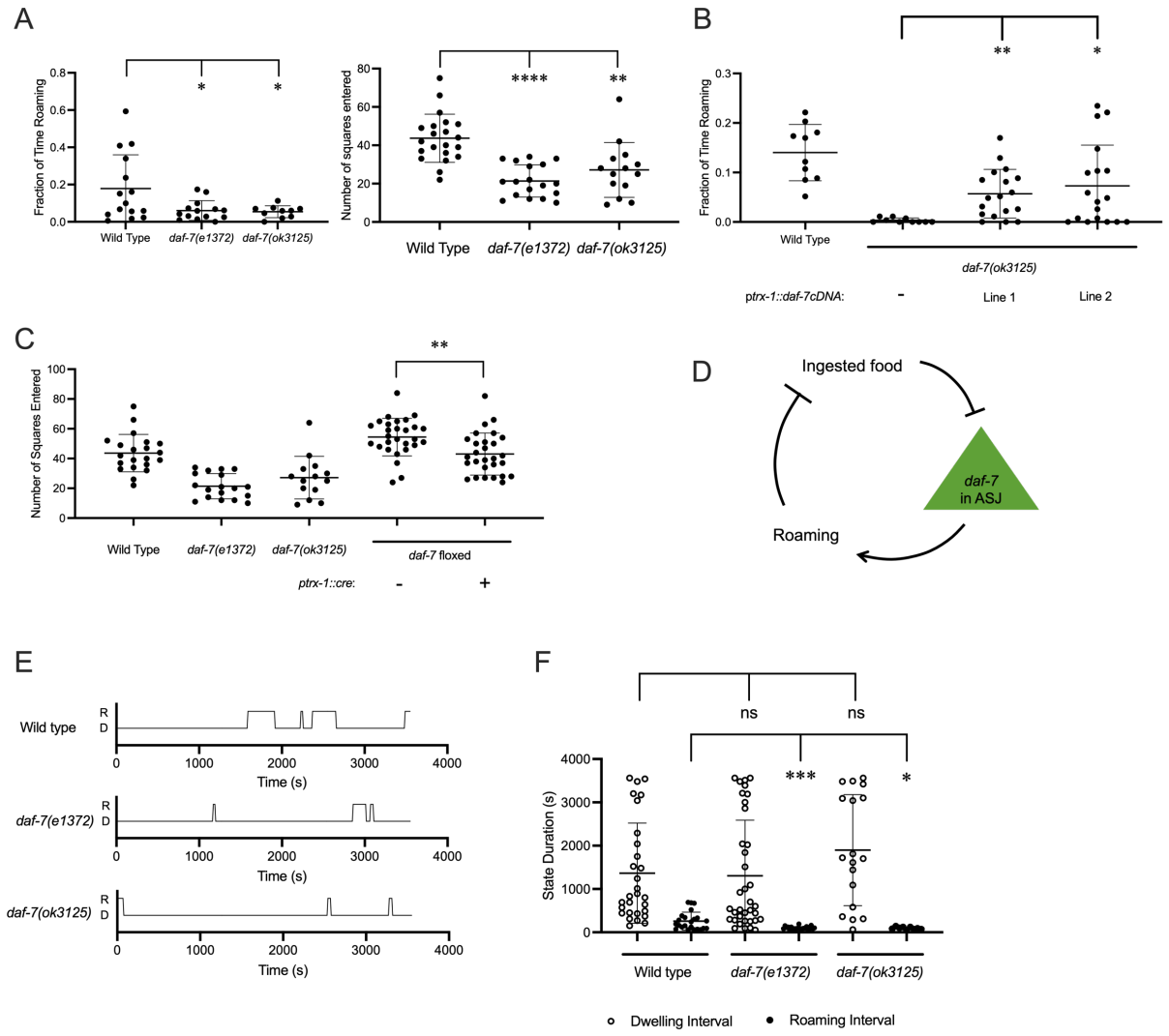

Figure 2. *daf-7* expression in the ASJ neurons promotes roaming.

A. Fraction of time roaming (left), and number of squares entered in exploration assay (right) of wild type, *daf-7(e1372)* and *daf-7(ok3125)* animals. Each point represents an individual animal, and error bars indicate standard deviation ****p<0.0001, **p<0.01, *p<0.05 as determined by an unpaired two-tailed t-test.

B. Fraction of time roaming of wild type, *daf-7(ok3125),* and two independent lines where *daf-7* cDNA was expressed under the *trx-1* promoter in a *daf-7(ok3125)* background.

497 Each point represents an individual animal, and error bars indicate standard deviation.
498 **p<0.01, *p<0.05 as determined by an unpaired two-tailed t-test.

499 C. Fraction of time roaming (left), and number of squares entered in exploration assay
500 (right) of wild type, *daf-7(e1372), daf-7(ok3125),* and a floxed *daf-7* strain with and
501 without Cre expressed under the *trx-1* promoter. Each point represents an individual
502 animal, and error bars indicate standard deviation. ** p<0.01, *p<0.05 as determined by
503 an unpaired two-tailed t-test.

504 D. Model of positive-feedback relationship between food ingestion, *daf-7* expression in the
505 ASJ neurons, and roaming.

506 E. Sample trace files of representative individual wild-type, *daf-7(e1372),* and *daf-*
507 *7(ok3125)* animals. R = roaming, D= dwelling.

508 F. Duration of dwelling (open circles) and roaming (closed circles) states for wild type, *daf-*
509 *7(e1372)* and *daf-7(ok3125)* animals. Each point represents a discrete roaming or
510 dwelling period. Error bars indicate standard deviation. ***p<0.001, *p<0.05, ns not
511 significant as determined by an unpaired two-tailed t-test.

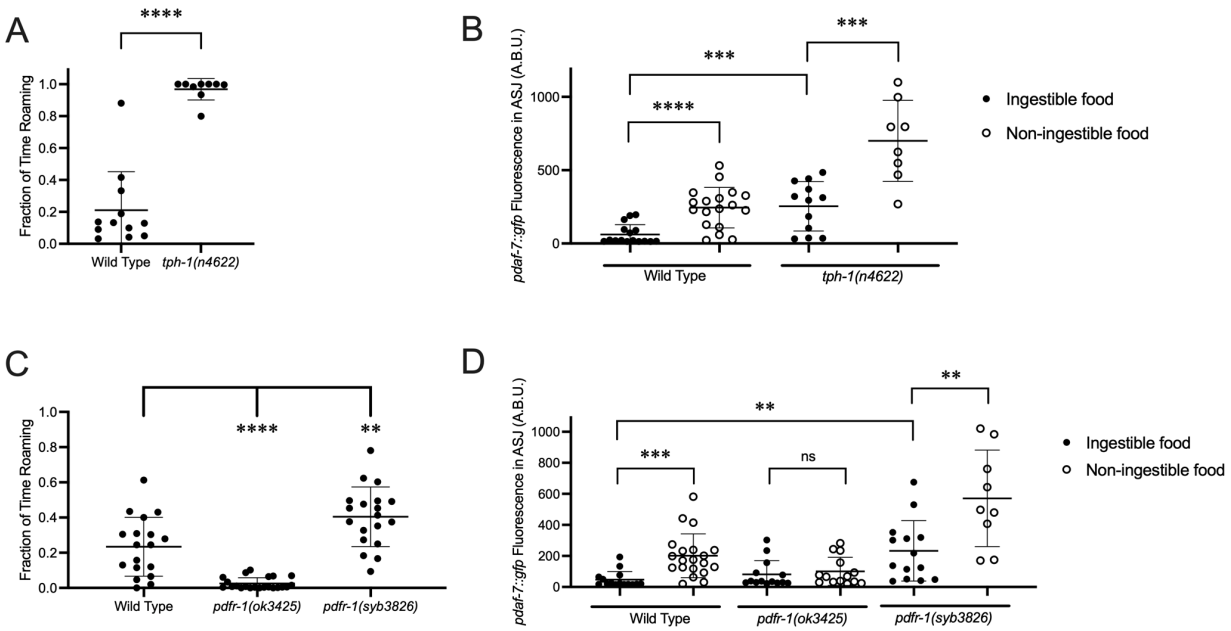

Figure 3. Known modulators of roaming and dwelling affect *daf-7* expression in the ASJ neurons

A. Fraction of time roaming of wild type and *tph-1(n4622)* animals. Each point represents an individual animal, and error bars indicate standard deviation. ****p<0.0001 as determined by an unpaired two-tailed t-test.

B. Maximum fluorescence values of *pdaf-7::gfp* in the ASJ neurons of adult wild type and *tph-1(n4622)* animals under "Fed" and "Bottom" conditions. Each point represents an individual animal, and error bars indicate standard deviation. ****p<0.0001, ***p<0.001 as determined by an unpaired two-tailed t-test.

C. Fraction of time roaming of wild type, *pdfr-1(ok3425),* and *pdfr-1(syb3826)* animals. Each point represents an individual animal, and error bars indicate standard deviation. ****p<0.0001, **p<0.01 as determined by an unpaired two-tailed t-test.

526 D. Maximum fluorescence values of *pdaf-7::gfp* in the ASJ neurons of adult wild type, *pdfr-*
527 *1(ok3425),* and *pdfr-1(syb3826)* animals under "Fed" and "Bottom" conditions. Each
528 point represents an individual animal, and error bars indicate standard deviation.
529 ***p<0.001, **p<0.01, ns not significant as determined by an unpaired two-tailed t-test.

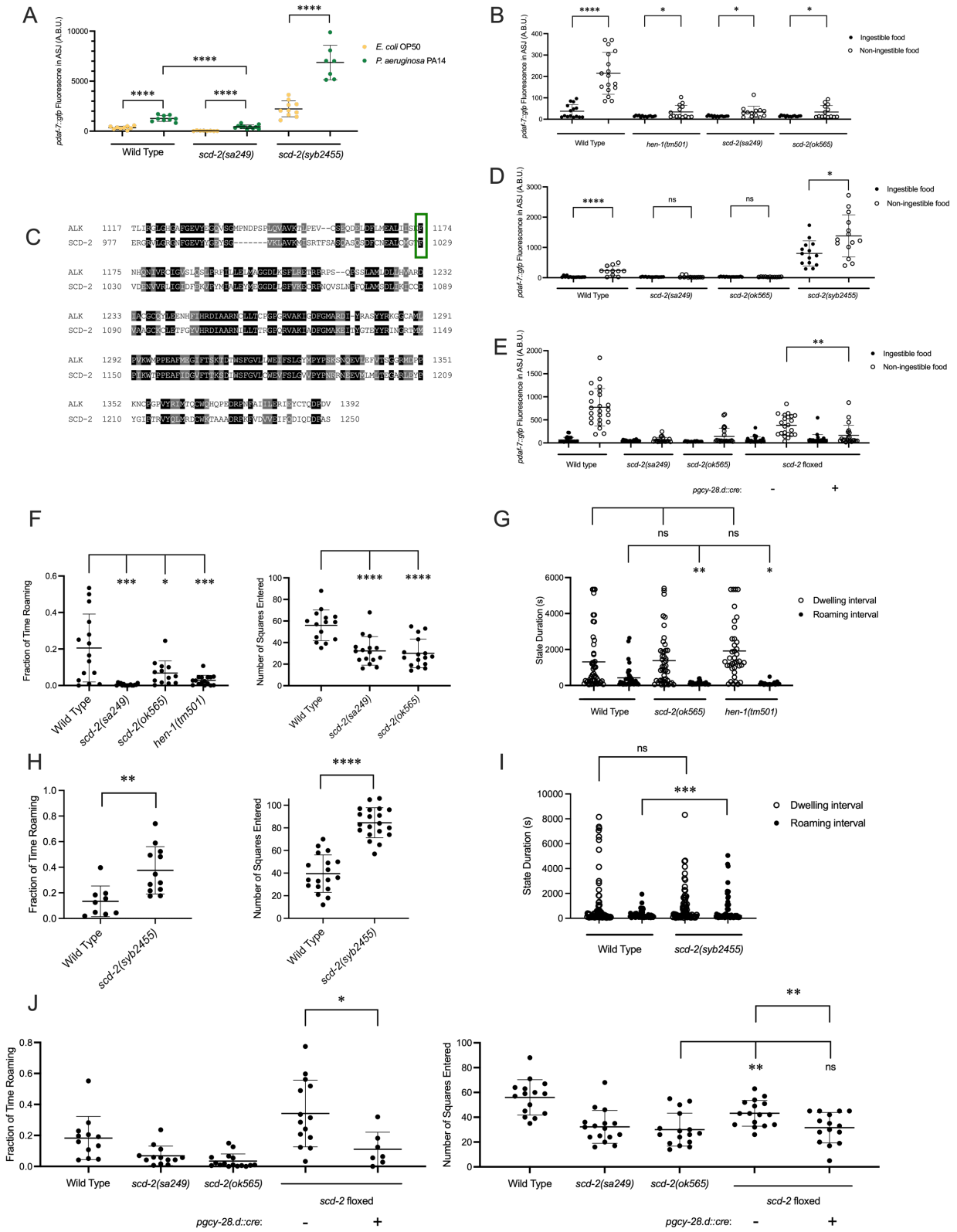

Figure 4. SCD-2 regulates *daf-7* expression in the ASJ neurons and roaming behavior

532 A. Maximum fluorescence values of *pdaf-7::gfp* in the ASJ neurons of adult wild type, *scd-*
533 *2(sa249),* and *scd-2(syb2455)* animals exposed to *E. coli* OP50 and *P. aeruginosa* PA14.
534 Each point represents an individual animal, and error bars indicate standard deviation.
535 ****p<0.0001, as determined by an unpaired two-tailed t-test.
536 B. Maximum fluorescence values of *pdaf-7::gfp* in the ASJ neurons of adult wild type, *hen-*
537 *1(tm501), scd-2(ok565)* and *scd-2(sa249)* animals under "Fed" and "Bottom" conditions.
538 Each point represents an individual animal, and error bars indicate standard deviation.
539 ****p<0.0001, *p<0.05 as determined by an unpaired two-tailed t-test.
540 C. Sequence alignment of the kinase domains of human ALK (top) and *C. elegans* SCD-2
541 (bottom). Amino acids highlighted in black are identical and those in gray are similar.
542 F1174/F1029 is outlined in green.
543 D. Maximum fluorescence values of *pdaf-7::gfp* in the ASJ neurons of adult wild type, *scd-*
544 *2(ok565), scd-2(sa249),* and *scd-2(syb2455)* animals under "Fed" and "Bottom"
545 conditions. Each point represents an individual animal, and error bars indicate standard
546 deviation. ****p<0.0001, *p<0.05, ns not significant as determined by an unpaired two-
547 tailed t-test.
548 E. Maximum fluorescence values of *pdaf-7::gfp* in the ASJ neurons of adult wild type,
549 floxed *scd-2, scd-2(sa249), scd-2(ok565),* and floxed *scd-2* animals with a transgene
550 expressing Cre under the AIA-specific *gcy-28.d* promoter under "Fed" and "Bottom"
551 conditions. Each point represents an individual animal, and error bars indicate standard
552 deviation. **p<0.01 as determined by an unpaired two-tailed t-test.
553 F. Fraction of time spent roaming (left) and number of squares entered in exploration assay
554 (right) for wild type, *scd-2(sa249), scd-2(ok565)* and *hen-1(tm501)* animals. Each point

555 represents an individual animal. Error bars indicate standard deviation. ****p<0.0001,
556 ***p<0.001, *p<0.05 as determined by an unpaired two-tailed t-test.
557 G. Duration of roaming (closed circles) and dwelling (open circles) states for wild type, *scd-*
558 *2(ok565)* and *hen-1(tm501*. Each point represents a discrete roaming or dwelling period.
559 Error bars indicate standard deviation. **p<0.01, *p<0.05, ns not significant as
560 determined by an unpaired two-tailed t-test.
561 H. Fraction of time spent roaming (left) and number of squares entered in exploration assay
562 (right) for wild type and *scd-2(syb2455)* animals. Each point represents an individual
563 animal. Error bars indicate standard deviation. ****p<0.0001, **p<0.01 as determined by
564 an unpaired two-tailed t-test.
565 I. Duration of roaming (closed circles) and dwelling (open circles) states for wild type and
566 *scd-2(syb2455)* animals. Each point represents a discrete roaming or dwelling period.
567 Error bars indicate standard deviation. ***p<0.001, ns not significant as determined by
568 an unpaired two-tailed t-test.
569 J. Left: Fraction of time spent roaming in worm tracker assay for *scd-2(sa249), scd-*
570 *2(ok565)* and floxed *scd-2* with or without a transgene expressing Cre under the AIA-
571 specific *gcy-28.d* promoter. Right: number of squares entered in exploration assay for
572 wild type, *scd-2(sa249), scd-2(ok565),* and floxed *scd-2* with or without a transgene
573 expressing Cre under the AIA-specific *gcy-28.d* promoter. Each point represents an
574 individual animal. Error bars indicate standard deviation. **p<0.01, *p<0.05, ns not
575 significant as determined by an unpaired two-tailed t-test.
576

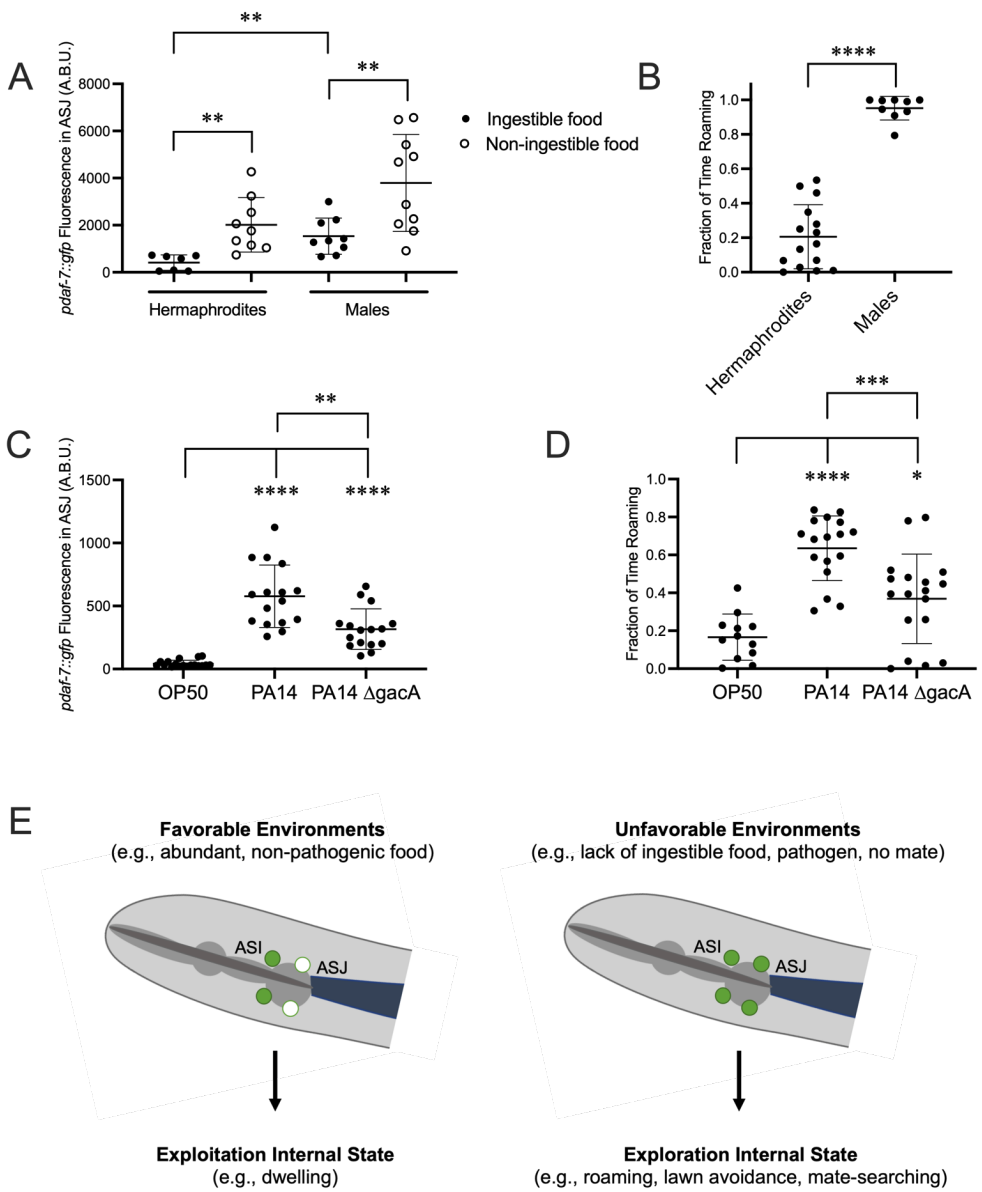

Figure 5. DAF-7 expression in the ASJ neurons correlates with an increase in roaming behavior under various conditions

A. Maximum fluorescence values of *pdaf-7::gfp* in the ASJ neurons of adult hermaphrodites and males under "Fed" and "Aztreonam" conditions. Each point represents an individual animal, and error bars indicate standard deviation. **p<0.01 as determined by an unpaired t-test.

584 B. Fraction of time roaming of wild-type hermaphrodites and males. Each point represents
585 an individual animal, and error bars indicate standard deviation. ****p<0.0001 as
586 determined by an unpaired t-test.
587 C. Maximum fluorescence values of *pdaf-7::gfp* in the ASJ neurons of adult hermaphrodites
588 fed *E. coli* OP50, *P. aeruginosa* PA14 or *P. aeruginosa* PA14ΔgacA. Each point
589 represents an individual animal, and error bars indicate standard deviation.
590 ****p<0.0001, **p<0.01 as determined by an unpaired t-test.
591 D. Fraction of time roaming of wild-type hermaphrodites on *E. coli* OP50, *P. aeruginosa*
592 PA14, or PA14 ΔgacA. Each point represents an individual animal, and error bars
593 indicate standard deviation. ****p<0.0001, ***p<0.001, *p<0.05 as determined by an
594 unpaired t-test.
595 E. *daf-7* expression in the ASJ neurons responds to environmental conditions and is
596 correlated with internal state. Under favorable conditions, *daf-7* is not expressed in the
597 ASJ neurons, and this is correlated with an internal state that favors exploitation of the
598 animal's current environment. Under unfavorable conditions, *daf-7* expression is induced
599 in the ASJ neurons, consistent with an internal state that favors exploration.

References

Bargmann, C. I. (2012). Beyond the connectome: how neuromodulators shape neural circuits. *Bioessays*, *34*(6), 458-465. https://doi.org/10.1002/bies.201100185

Ben Arous, J., Laffont, S., & Chatenay, D. (2009). Molecular and sensory basis of a food related two-state behavior in C. elegans. *PLoS One*, *4*(10), e7584. https://doi.org/10.1371/journal.pone.0007584

Boor, S. (2022). *Genetic Analysis of Bacterial Food Perception and its Influence on Foraging Behavior in C. elegans* Massachusetts Institute of Technology]. Cambridge, MA.

Brenner, S. (1974). The genetics of Caenorhabditis elegans. *Genetics*, *77*(1), 71-94. https://doi.org/10.1093/genetics/77.1.71

Chen, Y., Takita, J., Choi, Y. L., Kato, M., Ohira, M., Sanada, M., Wang, L., Soda, M., Kikuchi, A., Igarashi, T., Nakagawara, A., Hayashi, Y., Mano, H., & Ogawa, S. (2008). Oncogenic mutations of ALK kinase in neuroblastoma. *Nature*, *455*(7215), 971-974. https://doi.org/10.1038/nature07399

Cheng, L. Y., Bailey, A. P., Leevers, S. J., Ragan, T. J., Driscoll, P. C., & Gould, A. P. (2011). Anaplastic lymphoma kinase spares organ growth during nutrient restriction in Drosophila. *Cell*, *146*(3), 435-447. https://doi.org/10.1016/j.cell.2011.06.040

Churgin, M. A., McCloskey, R. J., Peters, E., & Fang-Yen, C. (2017). Antagonistic Serotonergic and Octopaminergic Neural Circuits Mediate Food-Dependent Locomotory Behavior in Caenorhabditis elegans. *J Neurosci*, *37*(33), 7811-7823. https://doi.org/10.1523/JNEUROSCI.2636-16.2017

Connolly, K. J. (1966). Locomotor activity in Drosophila as a function of food deprivation. *Nature*, *209*(5019), 224. https://doi.org/10.1038/209224a0

Dobosiewicz, M., Liu, Q., & Bargmann, C. I. (2019). Reliability of an interneuron response depends on an integrated sensory state. *Elife*, *8*. https://doi.org/10.7554/eLife.50566

Entchev, E. V., Patel, D. S., Zhan, M., Steele, A. J., Lu, H., & Ch'ng, Q. (2015). A gene-expression-based neural code for food abundance that modulates lifespan. *Elife*, *4*, e06259. https://doi.org/10.7554/eLife.06259

Flavell, S. W., Gogolla, N., Lovett-Barron, M., & Zelikowsky, M. (2022). The emergence and influence of internal states. *Neuron*, *110*(16), 2545-2570. https://doi.org/10.1016/j.neuron.2022.04.030

Flavell, S. W., Pokala, N., Macosko, E. Z., Albrecht, D. R., Larsch, J., & Bargmann, C. I. (2013). Serotonin and the neuropeptide PDF initiate and extend opposing behavioral states in C. elegans. *Cell*, *154*(5), 1023-1035. https://doi.org/10.1016/j.cell.2013.08.001

Flavell, S. W., Raizen, D. M., & You, Y. J. (2020). Behavioral States. *Genetics*, *216*(2), 315-332. https://doi.org/10.1534/genetics.120.303539

Franco, R., Rocco, G., Marino, F. Z., Pirozzi, G., Normanno, N., Morabito, A., Sperlongano, P., Stiuso, P., Luce, A., Botti, G., & Caraglia, M. (2013). Anaplastic lymphoma kinase: a glimmer of hope in lung cancer treatment? *Expert Rev Anticancer Ther*, *13*(4), 407-420. https://doi.org/10.1586/era.13.18

Fujiwara, M., Sengupta, P., & McIntire, S. L. (2002). Regulation of body size and behavioral state of C. elegans by sensory perception and the EGL-4 cGMP-dependent protein kinase. *Neuron*, *36*(6), 1091-1102. https://doi.org/10.1016/s0896-6273(02)01093-0

George, R. E., Sanda, T., Hanna, M., Frohling, S., Luther, W., 2nd, Zhang, J., Ahn, Y., Zhou, W., London, W. B., McGrady, P., Xue, L., Zozulya, S., Gregor, V. E., Webb, T. R., Gray, N. S., Gilliland, D. G., Diller, L., Greulich, H., Morris, S. W., . . . Look, A. T. (2008).

Activating mutations in ALK provide a therapeutic target in neuroblastoma. *Nature*, *455*(7215), 975-978. https://doi.org/10.1038/nature07397

Golden, J. W., & Riddle, D. L. (1982). A pheromone influences larval development in the nematode Caenorhabditis elegans. *Science*, *218*(4572), 578-580. https://doi.org/10.1126/science.6896933

Golden, J. W., & Riddle, D. L. (1984a). ACaenorhabditis elegans dauer-inducing pheromone and an antagonistic component of the food supply. *J Chem Ecol*, *10*(8), 1265-1280. https://doi.org/10.1007/BF00988553

Golden, J. W., & Riddle, D. L. (1984b). The Caenorhabditis elegans dauer larva: developmental effects of pheromone, food, and temperature. *Dev Biol*, *102*(2), 368-378. https://doi.org/10.1016/0012-1606(84)90201-x

Golden, J. W., & Riddle, D. L. (1984c). A pheromone-induced developmental switch in Caenorhabditis elegans: Temperature-sensitive mutants reveal a wild-type temperature-dependent process. *Proc Natl Acad Sci U S A*, *81*(3), 819-823. https://doi.org/10.1073/pnas.81.3.819

Greer, E. R., Perez, C. L., Van Gilst, M. R., Lee, B. H., & Ashrafi, K. (2008). Neural and molecular dissection of a C. elegans sensory circuit that regulates fat and feeding. *Cell Metab*, *8*(2), 118-131. https://doi.org/10.1016/j.cmet.2008.06.005

Gruninger, T. R., Gualberto, D. G., & Garcia, L. R. (2008). Sensory perception of food and insulin-like signals influence seizure susceptibility. *PLoS Genet*, *4*(7), e1000117. https://doi.org/10.1371/journal.pgen.1000117

Gutman, R., Yosha, D., Choshniak, I., & Kronfeld-Schor, N. (2007). Two strategies for coping with food shortage in desert golden spiny mice. *Physiol Behav*, *90*(1), 95-102. https://doi.org/10.1016/j.physbeh.2006.08.033

Hallberg, B., & Palmer, R. H. (2013). Mechanistic insight into ALK receptor tyrosine kinase in human cancer biology. *Nat Rev Cancer*, *13*(10), 685-700. https://doi.org/10.1038/nrc3580

Harris, N., Bates, S. G., Zhuang, Z., Bernstein, M., Stonemetz, J. M., Hill, T. J., Yu, Y. V., Calarco, J. A., & Sengupta, P. (2023). Molecular encoding of stimulus features in a single sensory neuron type enables neuronal and behavioral plasticity. *Curr Biol*, *33*(8), 1487-1501 e1487. https://doi.org/10.1016/j.cub.2023.02.073

Herbers, J. M. (1981). Time resources and laziness in animals. *Oecologia*, *49*(2), 252-262. https://doi.org/10.1007/BF00349198

Hilbert, Z. A., & Kim, D. H. (2017). Sexually dimorphic control of gene expression in sensory neurons regulates decision-making behavior in C. elegans. *Elife*, *6*. https://doi.org/10.7554/eLife.21166

Hilbert, Z. A., & Kim, D. H. (2018). PDF-1 neuropeptide signaling regulates sexually dimorphic gene expression in shared sensory neurons of C. elegans. *Elife*, *7*. https://doi.org/10.7554/eLife.36547

Holla, V. R., Elamin, Y. Y., Bailey, A. M., Johnson, A. M., Litzenburger, B. C., Khotskaya, Y. B., Sanchez, N. S., Zeng, J., Shufean, M. A., Shaw, K. R., Mendelsohn, J., Mills, G. B., Meric-Bernstam, F., & Simon, G. R. (2017). ALK: a tyrosine kinase target for cancer therapy. *Cold Spring Harb Mol Case Stud*, *3*(1), a001115. https://doi.org/10.1101/mcs.a001115

Inoue, T., & Thomas, J. H. (2000). Suppressors of transforming growth factor-beta pathway mutants in the Caenorhabditis elegans dauer formation pathway. *Genetics*, *156*(3), 1035-1046. https://doi.org/10.1093/genetics/156.3.1035

692 Ishihara, T., Iino, Y., Mohri, A., Mori, I., Gengyo-Ando, K., Mitani, S., & Katsura, I. (2002).
693 HEN-1, a secretory protein with an LDL receptor motif, regulates sensory integration and
694 learning in Caenorhabditis elegans. *Cell*, *109*(5), 639-649. https://doi.org/10.1016/s0092-
695 8674(02)00748-1
696 Iwahara, T., Fujimoto, J., Wen, D., Cupples, R., Bucay, N., Arakawa, T., Mori, S., Ratzkin, B.,
697 & Yamamoto, T. (1997). Molecular characterization of ALK, a receptor tyrosine kinase
698 expressed specifically in the nervous system. *Oncogene*, *14*(4), 439-449.
699 https://doi.org/10.1038/sj.onc.1200849
700 Janoueix-Lerosey, I., Lequin, D., Brugieres, L., Ribeiro, A., de Pontual, L., Combaret, V.,
701 Raynal, V., Puisieux, A., Schleiermacher, G., Pierron, G., Valteau-Couanet, D., Frebourg,
702 T., Michon, J., Lyonnet, S., Amiel, J., & Delattre, O. (2008). Somatic and germline
703 activating mutations of the ALK kinase receptor in neuroblastoma. *Nature*, *455*(7215),
704 967-970. https://doi.org/10.1038/nature07398
705 Ji, N., Madan, G. K., Fabre, G. I., Dayan, A., Baker, C. M., Kramer, T. S., Nwabudike, I., &
706 Flavell, S. W. (2021). A neural circuit for flexible control of persistent behavioral states.
707 *Elife*, *10*. https://doi.org/10.7554/eLife.62889
708 Johnson, R. E., Linderman, S., Panier, T., Wee, C. L., Song, E., Herrera, K. J., Miller, A., &
709 Engert, F. (2020). Probabilistic Models of Larval Zebrafish Behavior Reveal Structure on
710 Many Scales. *Curr Biol*, *30*(1), 70-82 e74. https://doi.org/10.1016/j.cub.2019.11.026
711 Kim, D. H., & Flavell, S. W. (2020). Host-microbe interactions and the behavior of
712 Caenorhabditis elegans. *J Neurogenet*, *34*(3-4), 500-509.
713 https://doi.org/10.1080/01677063.2020.1802724
714 Kyani-Rogers, T., Philbrook, A., McLachlan, I. G., Flavell, S. W., O'Donnell, M. P., &
715 Sengupta, P. (2022). Developmental history modulates adult olfactory behavioral
716 preferences via regulation of chemoreceptor expression in Caenorhabditiselegans.
717 *Genetics*, *222*(3). https://doi.org/10.1093/genetics/iyac143
718 McLachlan, I. G., Kramer, T. S., Dua, M., DiLoreto, E. M., Gomes, M. A., Dag, U., Srinivasan,
719 J., & Flavell, S. W. (2022). Diverse states and stimuli tune olfactory receptor expression
720 levels to modulate food-seeking behavior. *Elife*, *11*. https://doi.org/10.7554/eLife.79557
721 Meisel, J. D., Panda, O., Mahanti, P., Schroeder, F. C., & Kim, D. H. (2014). Chemosensation of
722 bacterial secondary metabolites modulates neuroendocrine signaling and behavior of C.
723 elegans. *Cell*, *159*(2), 267-280. https://doi.org/10.1016/j.cell.2014.09.011
724 Morris, S. W., Kirstein, M. N., Valentine, M. B., Dittmer, K. G., Shapiro, D. N., Saltman, D. L.,
725 & Look, A. T. (1994). Fusion of a kinase gene, ALK, to a nucleolar protein gene, NPM,
726 in non-Hodgkin's lymphoma. *Science*, *263*(5151), 1281-1284.
727 https://doi.org/10.1126/science.8122112
728 Oranth, A., Schultheis, C., Tolstenkov, O., Erbguth, K., Nagpal, J., Hain, D., Brauner, M.,
729 Wabnig, S., Steuer Costa, W., McWhirter, R. D., Zels, S., Palumbos, S., Miller Iii, D. M.,
730 Beets, I., & Gottschalk, A. (2018). Food Sensation Modulates Locomotion by Dopamine
731 and Neuropeptide Signaling in a Distributed Neuronal Network. *Neuron*, *100*(6), 1414-
732 1428 e1410. https://doi.org/10.1016/j.neuron.2018.10.024
733 Orthofer, M., Valsesia, A., Magi, R., Wang, Q. P., Kaczanowska, J., Kozieradzki, I., Leopoldi,
734 A., Cikes, D., Zopf, L. M., Tretiakov, E. O., Demetz, E., Hilbe, R., Boehm, A., Ticevic,
735 M., Noukas, M., Jais, A., Spirk, K., Clark, T., Amann, S., . . . Penninger, J. M. (2020).
736 Identification of ALK in Thinness. *Cell*, *181*(6), 1246-1262 e1222.
737 https://doi.org/10.1016/j.cell.2020.04.034

Overton, J. M., & Williams, T. D. (2004). Behavioral and physiologic responses to caloric restriction in mice. *Physiol Behav*, *81*(5), 749-754. https://doi.org/10.1016/j.physbeh.2004.04.025

Pradhan, S., Quilez, S., Homer, K., & Hendricks, M. (2019). Environmental Programming of Adult Foraging Behavior in C. elegans. *Curr Biol*, *29*(17), 2867-2879 e2864. https://doi.org/10.1016/j.cub.2019.07.045

Reiner, D. J., Ailion, M., Thomas, J. H., & Meyer, B. J. (2008). C. elegans anaplastic lymphoma kinase ortholog SCD-2 controls dauer formation by modulating TGF-beta signaling. *Curr Biol*, *18*(15), 1101-1109. https://doi.org/10.1016/j.cub.2008.06.060

Ren, P., Lim, C. S., Johnsen, R., Albert, P. S., Pilgrim, D., & Riddle, D. L. (1996). Control of C. elegans larval development by neuronal expression of a TGF-beta homolog. *Science*, *274*(5291), 1389-1391. https://doi.org/10.1126/science.274.5291.1389

Rhoades, J. L., Nelson, J. C., Nwabudike, I., Yu, S. K., McLachlan, I. G., Madan, G. K., Abebe, E., Powers, J. R., Colon-Ramos, D. A., & Flavell, S. W. (2019). ASICs Mediate Food Responses in an Enteric Serotonergic Neuron that Controls Foraging Behaviors. *Cell*, *176*(1-2), 85-97 e14. https://doi.org/10.1016/j.cell.2018.11.023

Russell, J. C., Epling, W. F., Pierce, D., Amy, R. M., & Boer, D. P. (1987). Induction of voluntary prolonged running by rats. *J Appl Physiol (1985)*, *63*(6), 2549-2553. https://doi.org/10.1152/jappl.1987.63.6.2549

Ryan, D. A., Miller, R. M., Lee, K., Neal, S. J., Fagan, K. A., Sengupta, P., & Portman, D. S. (2014). Sex, age, and hunger regulate behavioral prioritization through dynamic modulation of chemoreceptor expression. *Curr Biol*, *24*(21), 2509-2517. https://doi.org/10.1016/j.cub.2014.09.032

Sawin, E. R., Ranganathan, R., & Horvitz, H. R. (2000). C. elegans locomotory rate is modulated by the environment through a dopaminergic pathway and by experience through a serotonergic pathway. *Neuron*, *26*(3), 619-631. https://doi.org/10.1016/s0896-6273(00)81199-x

Schackwitz, W. S., Inoue, T., & Thomas, J. H. (1996). Chemosensory neurons function in parallel to mediate a pheromone response in C. elegans. *Neuron*, *17*(4), 719-728. https://doi.org/10.1016/s0896-6273(00)80203-2

Sengupta, P. (2013). The belly rules the nose: feeding state-dependent modulation of peripheral chemosensory responses. *Curr Opin Neurobiol*, *23*(1), 68-75. https://doi.org/10.1016/j.conb.2012.08.001

Shaw, W. M., Luo, S., Landis, J., Ashraf, J., & Murphy, C. T. (2007). The C. elegans TGF-beta Dauer pathway regulates longevity via insulin signaling. *Curr Biol*, *17*(19), 1635-1645. https://doi.org/10.1016/j.cub.2007.08.058

Shinkai, Y., Yamamoto, Y., Fujiwara, M., Tabata, T., Murayama, T., Hirotsu, T., Ikeda, D. D., Tsunozaki, M., Iino, Y., Bargmann, C. I., Katsura, I., & Ishihara, T. (2011). Behavioral choice between conflicting alternatives is regulated by a receptor guanylyl cyclase, GCY-28, and a receptor tyrosine kinase, SCD-2, in AIA interneurons of Caenorhabditis elegans. *J Neurosci*, *31*(8), 3007-3015. https://doi.org/10.1523/JNEUROSCI.4691-10.2011

Wexler, L. R., Miller, R. M., & Portman, D. S. (2020). C. elegans Males Integrate Food Signals and Biological Sex to Modulate State-Dependent Chemosensation and Behavioral Prioritization. *Curr Biol*, *30*(14), 2695-2706 e2694. https://doi.org/10.1016/j.cub.2020.05.006

White, J. G., Southgate, E., Thomson, J. N., & Brenner, S. (1986). The structure of the nervous system of the nematode Caenorhabditis elegans. *Philos Trans R Soc Lond B Biol Sci*, *314*(1165), 1-340. https://doi.org/10.1098/rstb.1986.0056

Wolfe, G. S., Tong, V. W., Povse, E., Merritt, D. M., Stegeman, G. W., Flibotte, S., & van der Kooy, D. (2019). A Receptor Tyrosine Kinase Plays Separate Roles in Sensory Integration and Associative Learning in C. elegans. *eNeuro*, *6*(4). https://doi.org/10.1523/ENEURO.0244-18.2019

Woodling, N. S., Aleyakpo, B., Dyson, M. C., Minkley, L. J., Rajasingam, A., Dobson, A. J., Leung, K. H. C., Pomposova, S., Fuentealba, M., Alic, N., & Partridge, L. (2020). The neuronal receptor tyrosine kinase Alk is a target for longevity. *Aging Cell*, *19*(5), e13137. https://doi.org/10.1111/acel.13137

WormLab. In. (2020). MBF Bioscience.

Yap, E. L., & Greenberg, M. E. (2018). Activity-Regulated Transcription: Bridging the Gap between Neural Activity and Behavior. *Neuron*, *100*(2), 330-348. https://doi.org/10.1016/j.neuron.2018.10.013

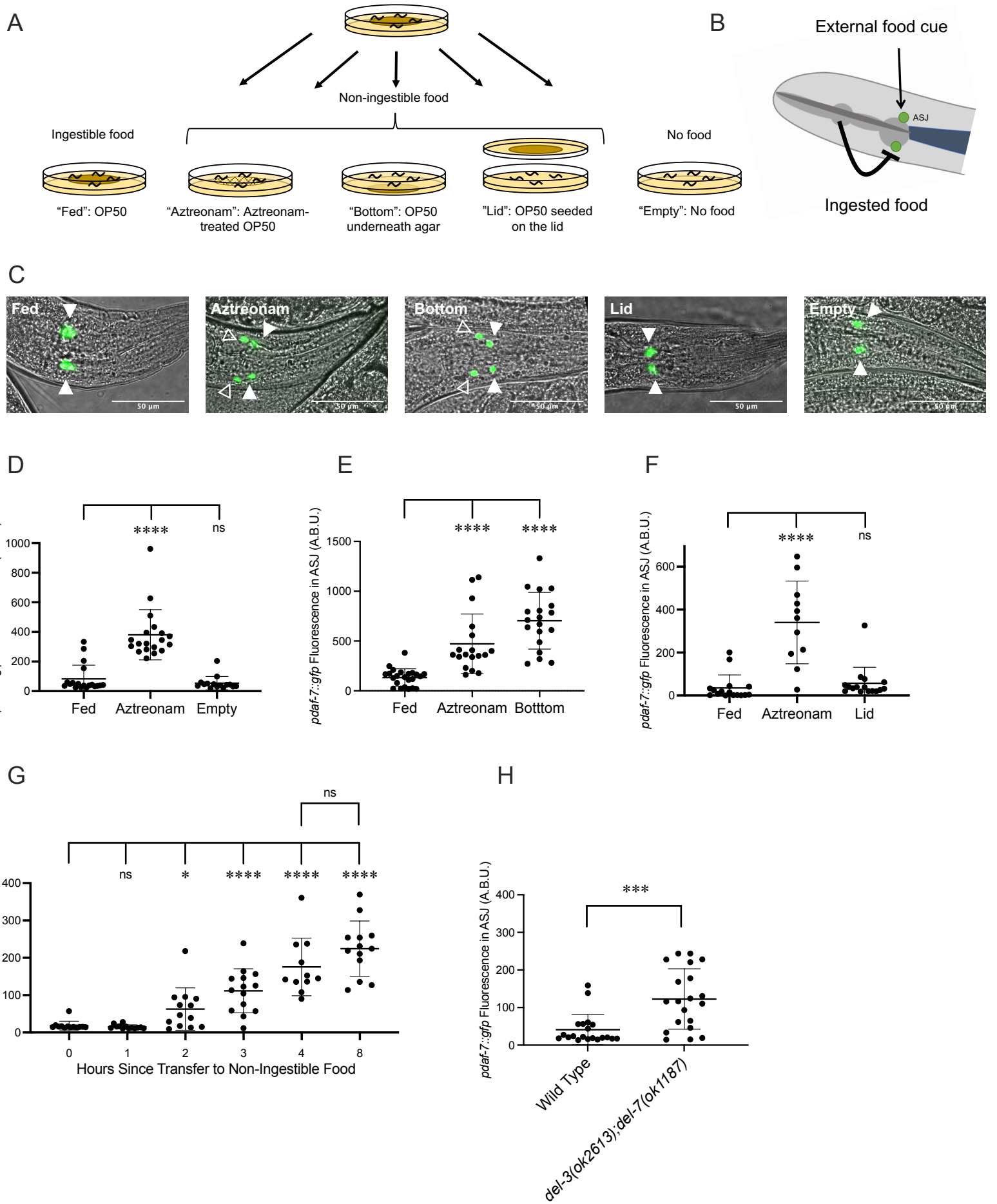
A
Non-ingestible food
Ingestible food
No food
"Fed": OP50
"Aztreonam": Aztreonam-treated OP50
"Bottom": OP50 underneath agar
"Lid": OP50 seeded on the lid
"Empty": No food
B
External food cue
ASJ
Ingested food
C
Fed
Aztreonam
Bottom
Lid
Empty
50 µm
D
pdaf-7::gfp Fluorescence in ASJ (A.B.U.)
****
ns
Fed
Aztreonam
Empty
E
pdaf-7::gfp Fluorescence in ASJ (A.B.U.)
****
****
Fed
Aztreonam
Botttom
F
pdaf-7::gfp Fluorescence in ASJ (A.B.U.)
****
ns
Fed
Aztreonam
Lid
G
pdaf-7::gfp Fluorescence in ASJ (A.B.U.)
ns
ns
*
****
****
****
Hours Since Transfer to Non-Ingestible Food
H
pdaf-7::gfp Fluorescence in ASJ (A.B.U.)
***
Wild Type
del-3(ok2613);del-7(ok1187)

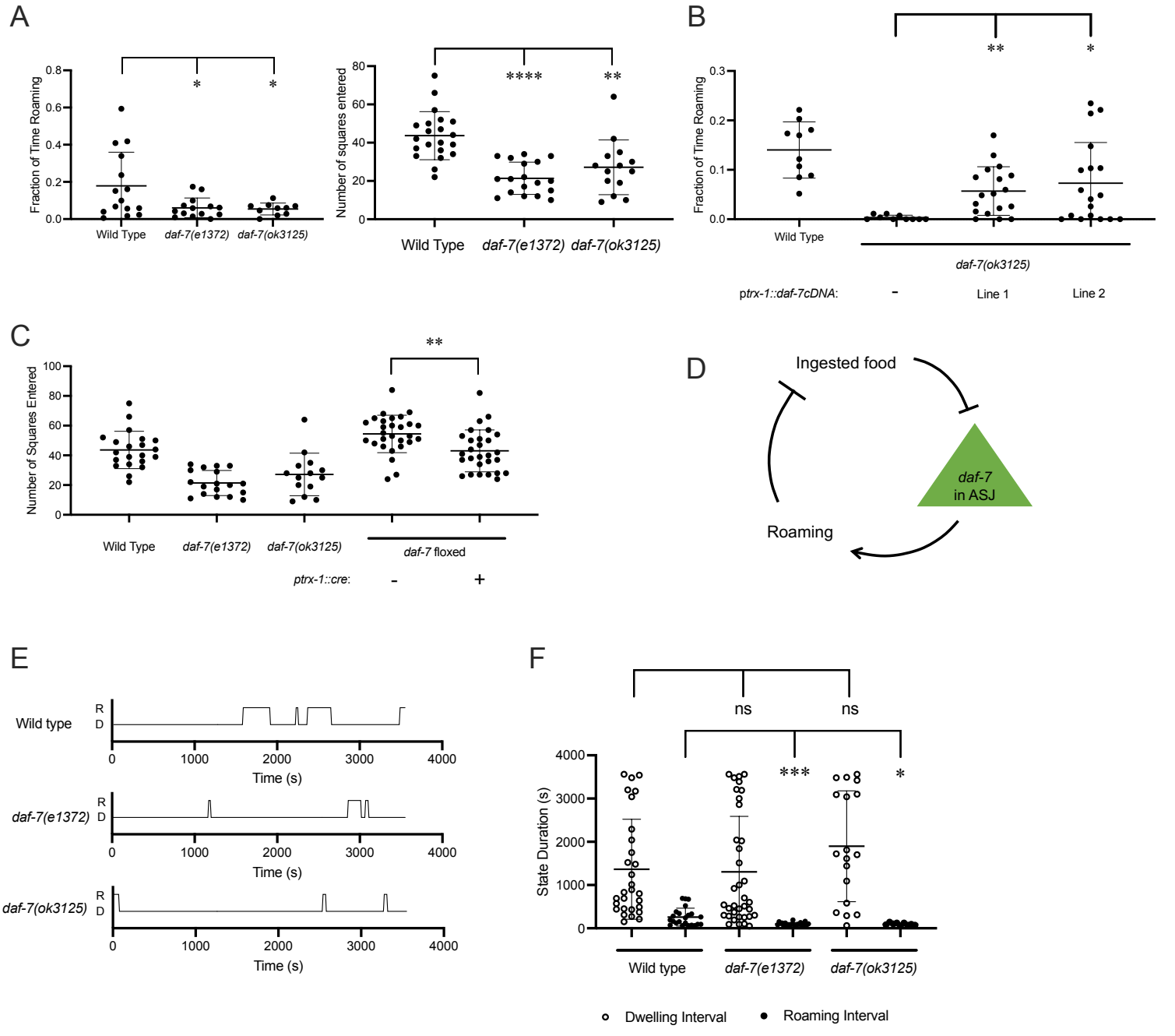
A
Fraction of Time Roaming
0.8
0.6
0.4
0.2
0.0
*
*
Wild Type
daf-7(e1372)
daf-7(ok3125)
Number of squares entered
80
60
40
20
0
****
**
Wild Type
daf-7(e1372)
daf-7(ok3125)
B
Fraction of Time Roaming
0.3
0.2
0.1
0.0
**
*
Wild Type
daf-7(ok3125)
ptrx-1::daf-7cDNA:
-
Line 1
Line 2
C
Number of Squares Entered
100
80
60
40
20
0
**
Wild Type
daf-7(e1372)
daf-7(ok3125)
daf-7 floxed
ptrx-1::cre:
-
+
D
Ingested food
daf-7
in ASJ
Roaming
E
Wild type
daf-7(e1372)
daf-7(ok3125)
R
D
0
1000
2000
3000
4000
Time (s)
F
ns
ns
***
*
State Duration (s)
4000
3000
2000
1000
0
Wild type
daf-7(e1372)
daf-7(ok3125)
Dwelling Interval
Roaming Interval

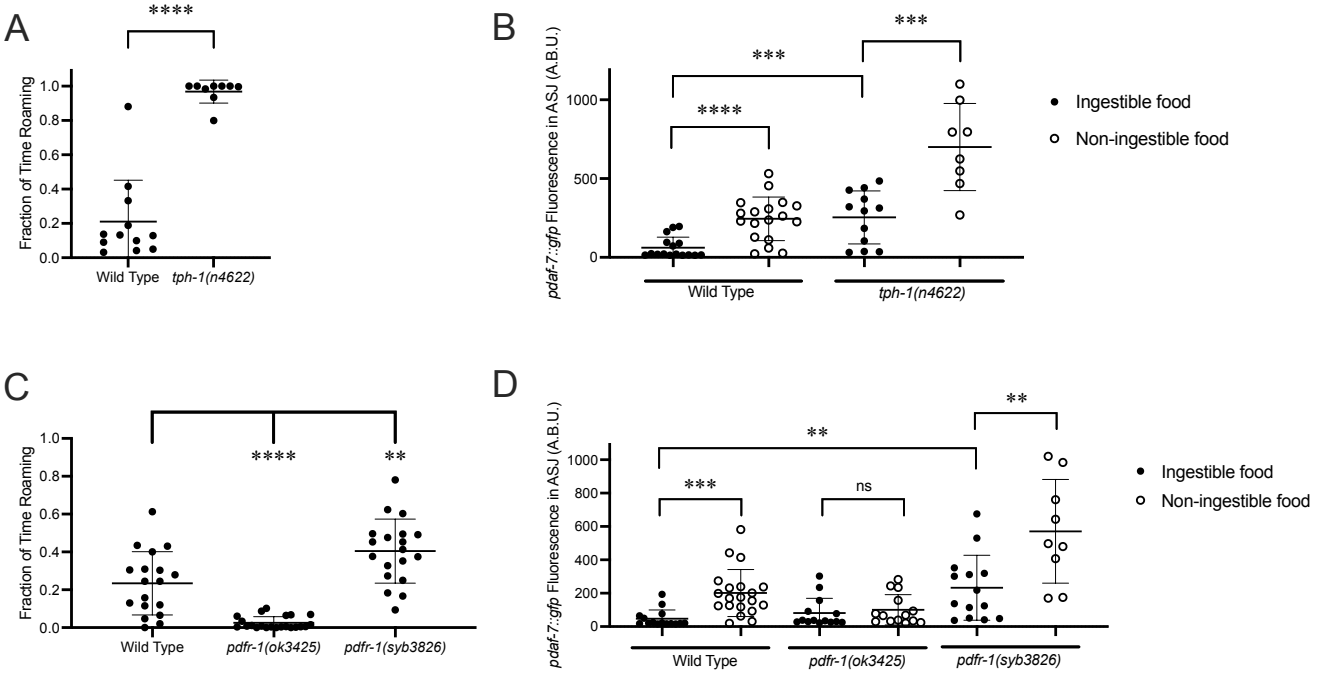
A
****
Fraction of Time Roaming
1.0
0.8
0.6
0.4
0.2
0.0
Wild Type
tph-1(n4622)
B
***
***
****
pdaf-7::gfp Fluorescence in ASJ (A.B.U.)
1000
500
0
Wild Type
tph-1(n4622)
Ingestible food
Non-ingestible food
C
****
**
Fraction of Time Roaming
1.0
0.8
0.6
0.4
0.2
0.0
Wild Type
pdfr-1(ok3425)
pdfr-1(syb3826)
D
**
**
***
ns
pdaf-7::gfp Fluorescence in ASJ (A.B.U.)
1000
800
600
400
200
0
Wild Type
pdfr-1(ok3425)
pdfr-1(syb3826)
Ingestible food
Non-ingestible food

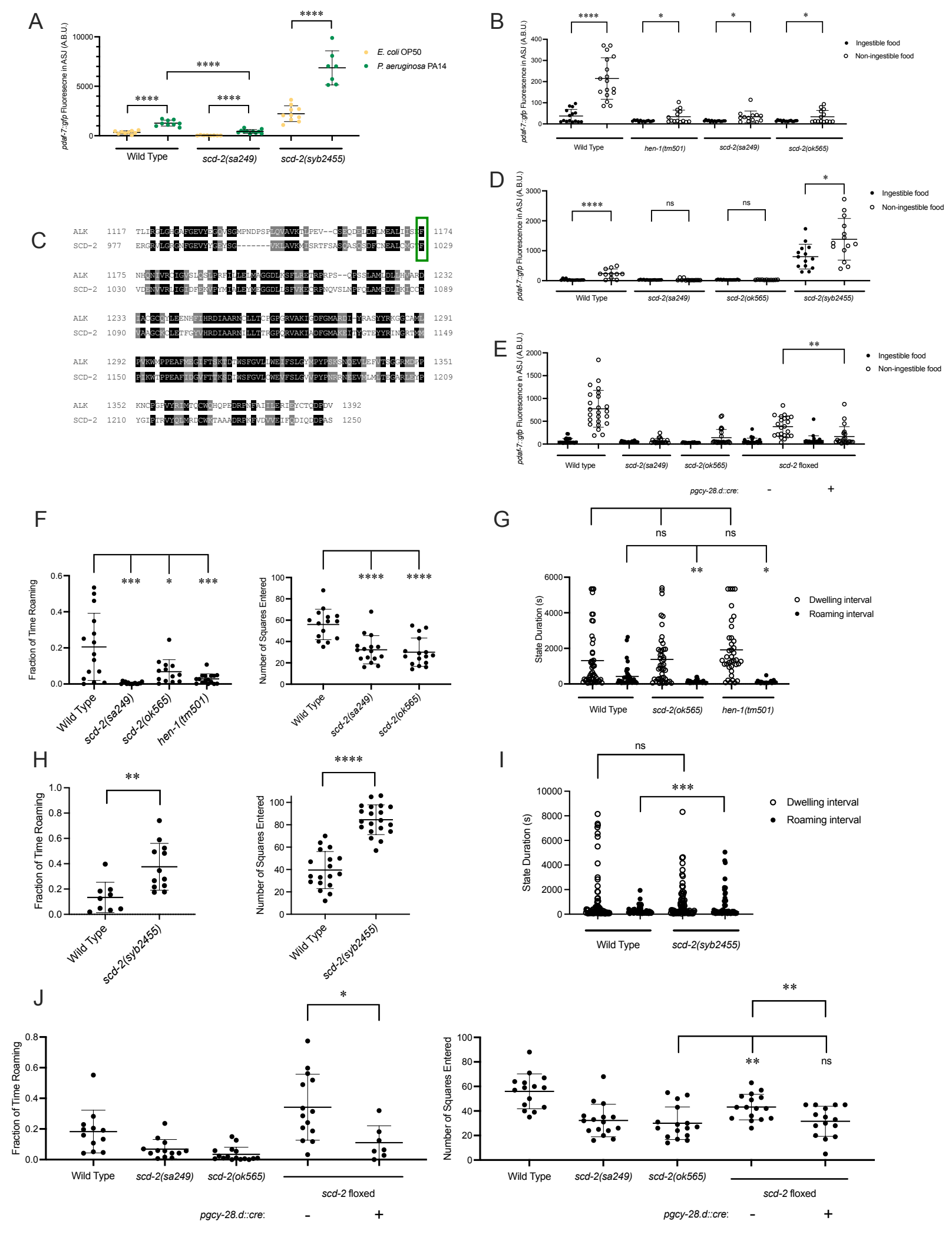
A
pdaf-7::gfp Fluorescence in ASJ (A.B.U.)
E. coli OP50
P. aeruginosa PA14
Wild Type
scd-2(sa249)
scd-2(syb2455)
B
Ingestible food
Non-ingestible food
hen-1(tm501)
scd-2(ok565)
C
ALK
SCD-2
D
ns
E
scd-2 floxed
pgcy-28.d::cre:
F
Fraction of Time Roaming
Number of Squares Entered
G
State Duration (s)
Dwelling interval
Roaming interval
H
I
J

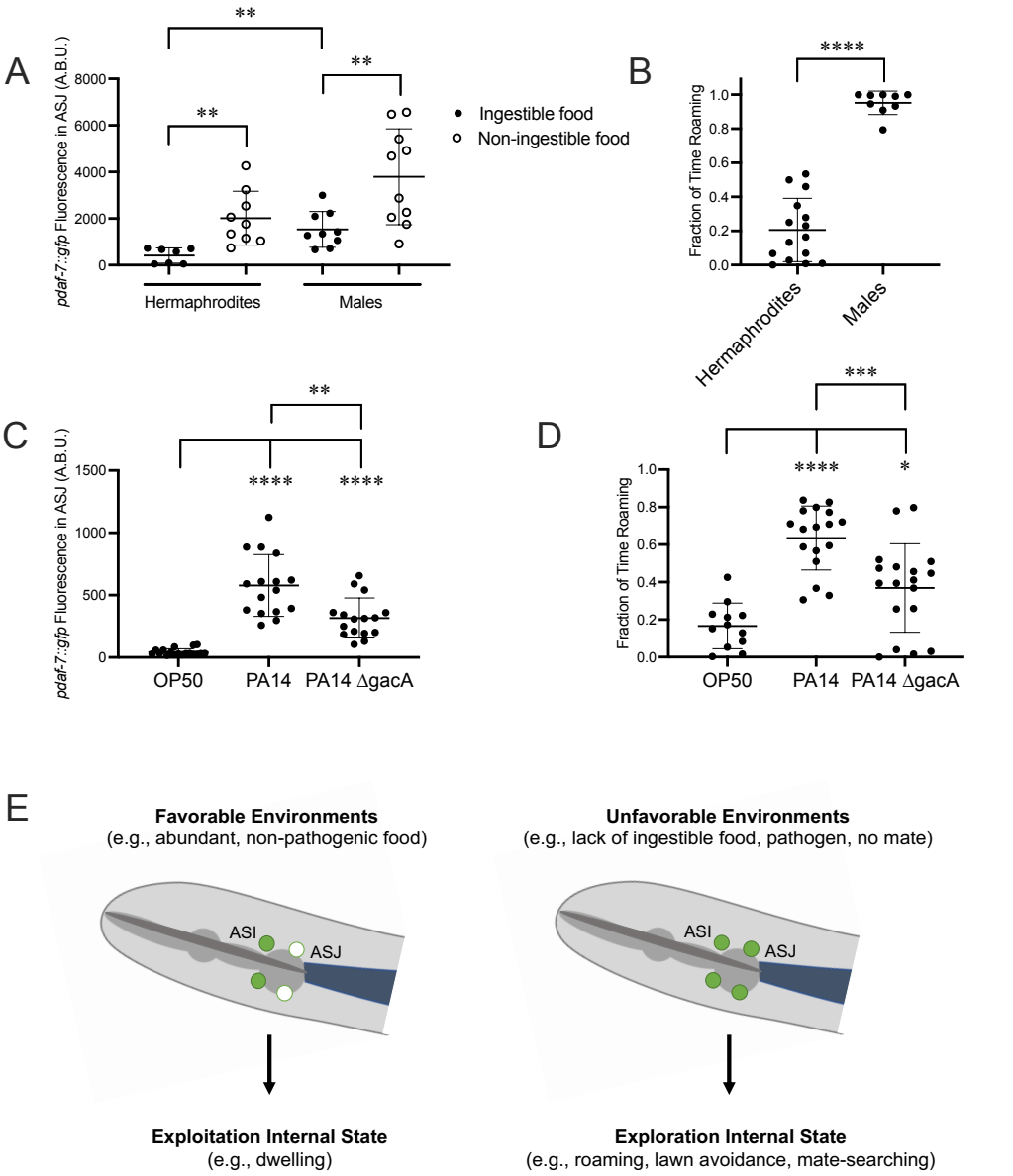
A
pdaf-7::gfp Fluorescence in ASJ (A.B.U.)
8000
6000
4000
2000
0
**
**
**
Ingestible food
Non-ingestible food
Hermaphrodites
Males
B
Fraction of Time Roaming
1.0
0.8
0.6
0.4
0.2
0.0
****
Hermaphrodites
Males
C
pdaf-7::gfp Fluorescence in ASJ (A.B.U.)
1500
1000
500
0
**
****
****
OP50
PA14
PA14 ΔgacA
D
Fraction of Time Roaming
1.0
0.8
0.6
0.4
0.2
0.0
***
****
*
OP50
PA14
PA14 ΔgacA
E
Favorable Environments
(e.g., abundant, non-pathogenic food)
ASI
ASJ
Exploitation Internal State
(e.g., dwelling)
Unfavorable Environments
(e.g., lack of ingestible food, pathogen, no mate)
ASI
ASJ
Exploration Internal State
(e.g., roaming, lawn avoidance, mate-searching)